

*Ultimate Lithography and Nanofabrication for Electronics and Life Science,
Marseille, June, 2006*

AFM Based Diagnostic and Lithography of Semiconductor Nanostructures

Alexander Latyshev and Dmitry Sheglov

**Institute of Semiconductor Physics, Novosibirsk, Russia
Novosibirsk State University, Physics Department, Russia**



Laboratory of Electron Microscopy and Submicron Structures

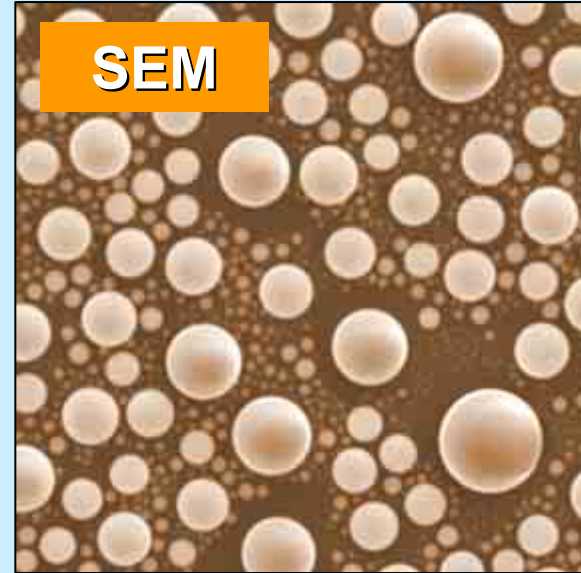
OUT-LINE

- **Nanostructure Fabrication by Lithography** (*optical and electron beam lithography, AFM based nanolithography*)
- **Methods of Atomic Manipulations** (*atomic processes at surface, interface and bulk, MBE, self-organization et al.*)
- **Diagnostics of Low-Dimension Systems with Atomic Resolution** (*HREM, SEM, AFM, STM, unique UHV-REM, ex- and in situ characterizations*)



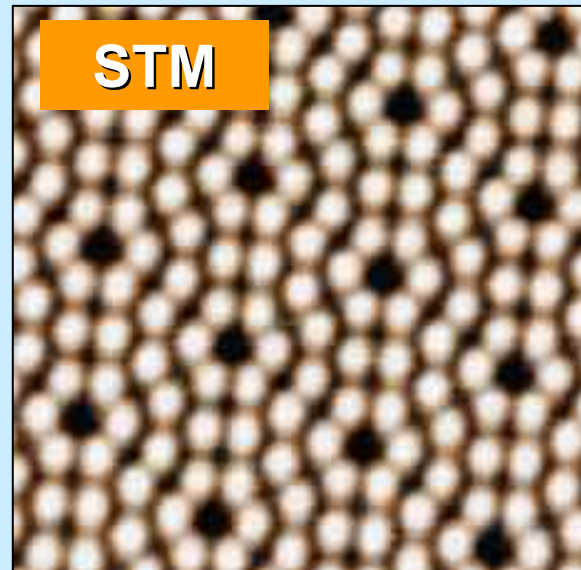
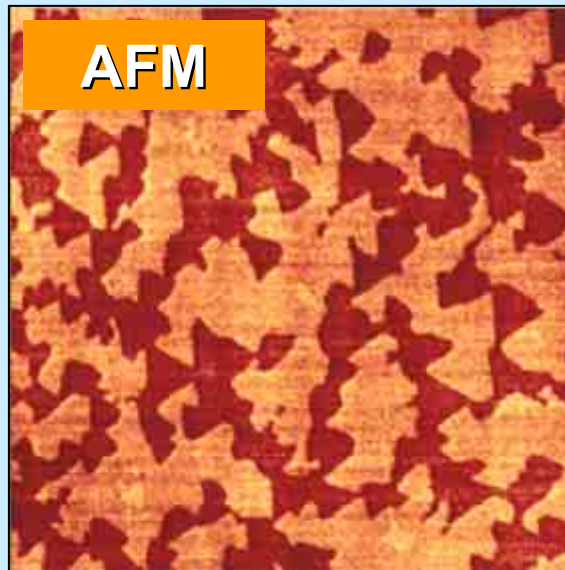
Imaging Techniques for Nanodiagnosics

Silicon,
JEM-4000EX,
(A.Gutakovskii)



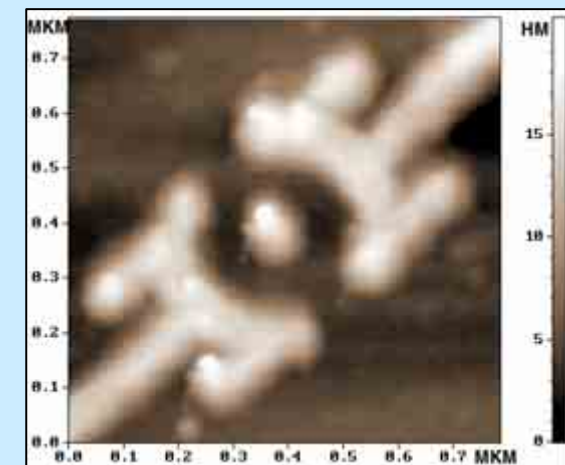
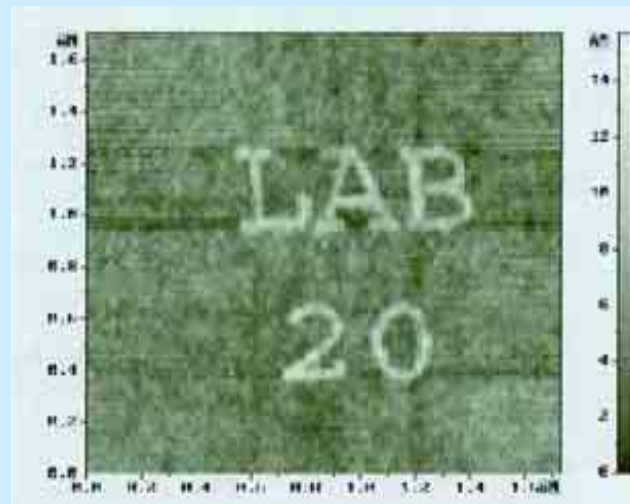
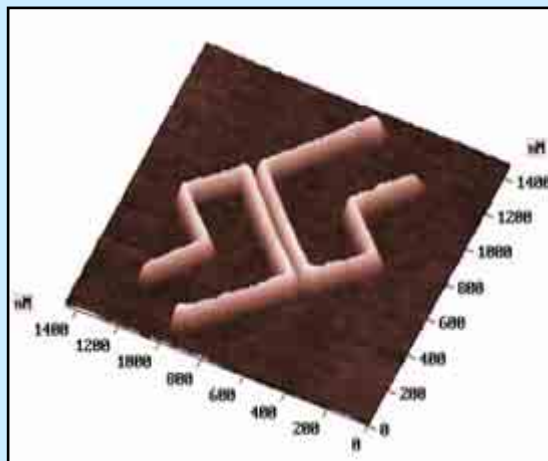
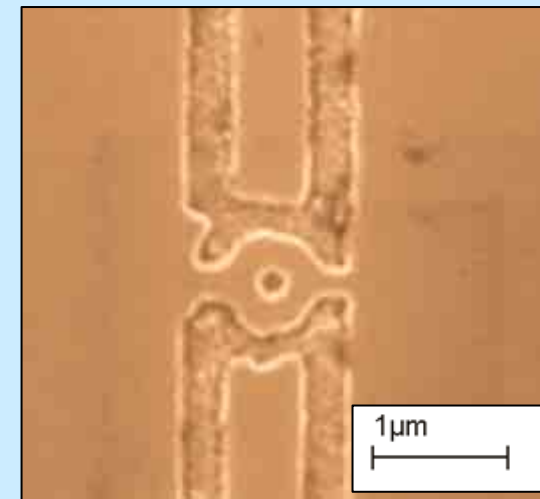
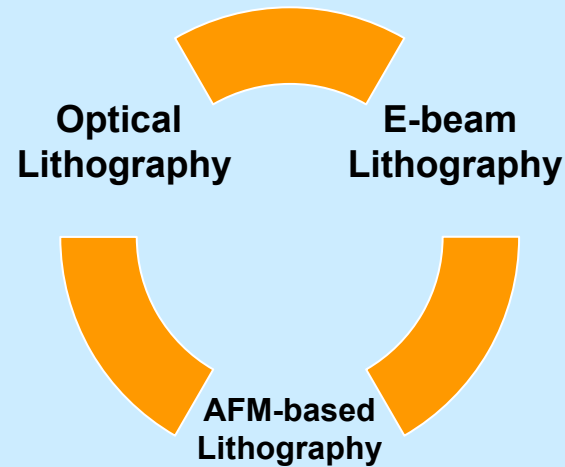
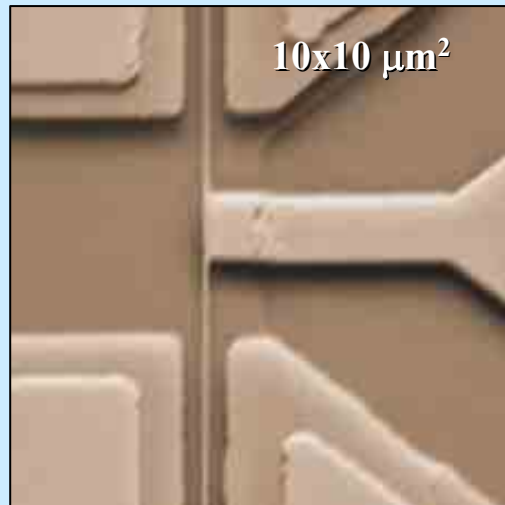
Au particles
on graphite,
LEO-1430,
(T.Gavrilova)

Si(111),
2D-islands
NT-MDT,
(E.Rodyakina)



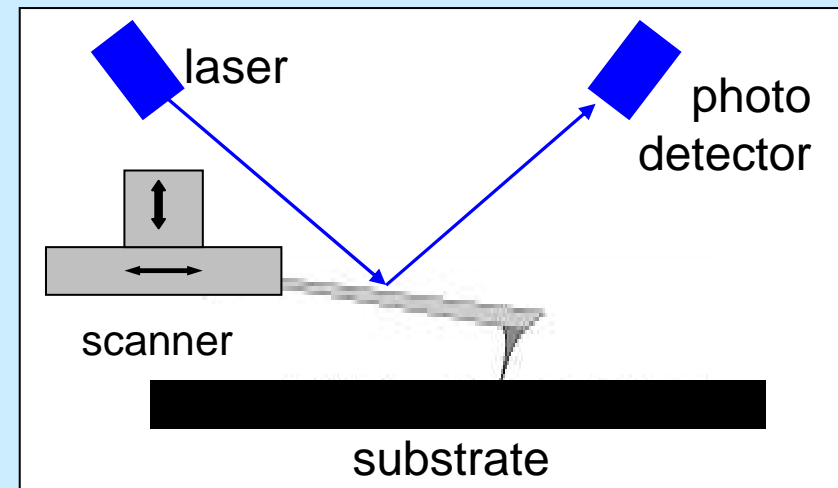
Si(111)
(7x7)
reconstruction,
Omicron,
(S.Teys)

Nano-Scaled Lithography



Atomic Force Microscope SOLVER P-47H (NT-MDT)

- For stability reasons, stiff cantilevers were preferable minimizing the effects of tip-substrate forces.
- To reduce noise contribution of external electromagnetic fields, the AFM apparatus have been positioned inside of a metal box having a good electric connection to ground.
- Additional rubber bearers for this box have been installed reducing mechanical vibration noise.
- The both temperature and humidity of atmosphere inside of the box were controlled during AFM scanning.



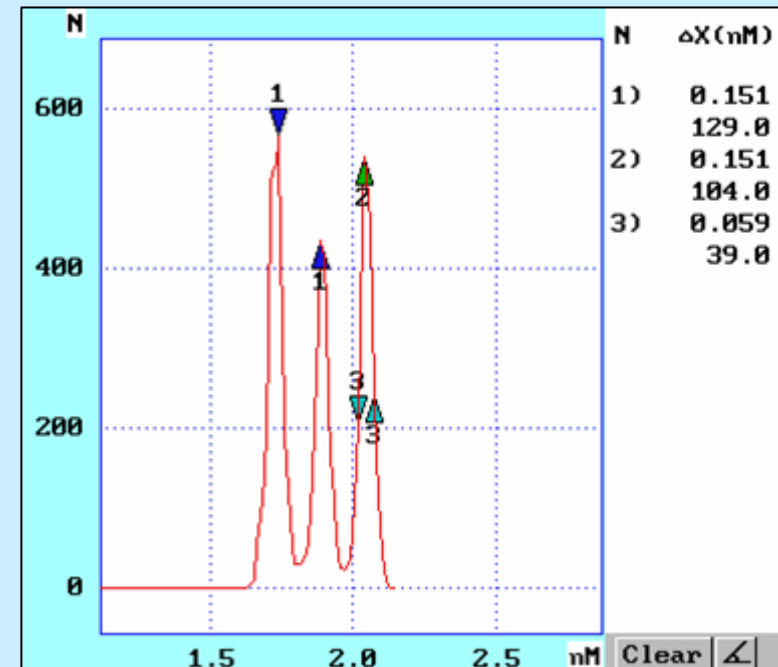
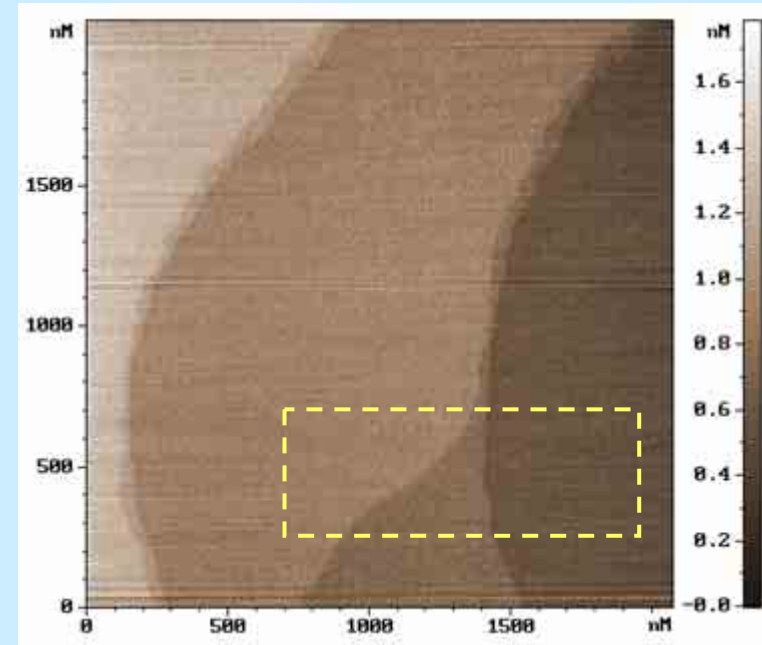
The both contact and semi-contact (frequency-modulation) modes were performed.

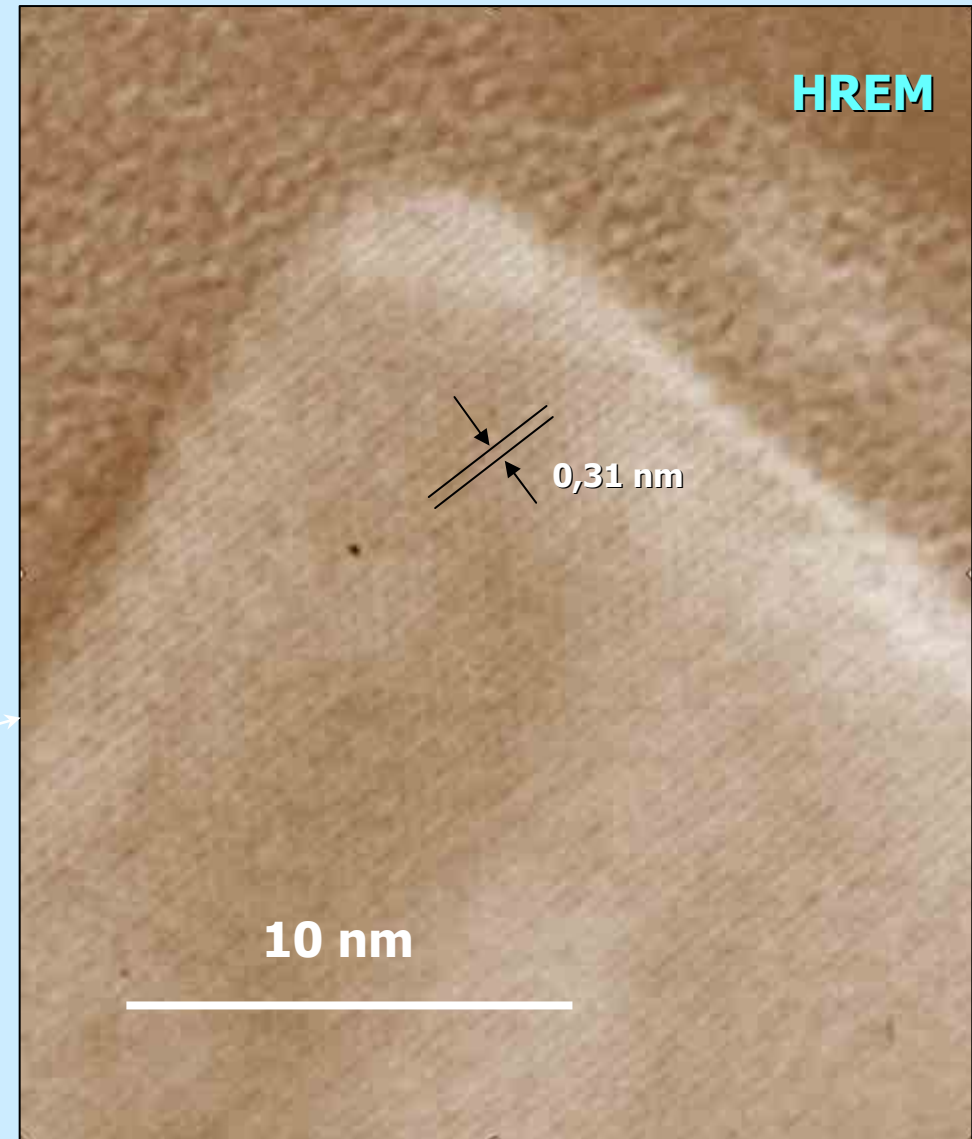
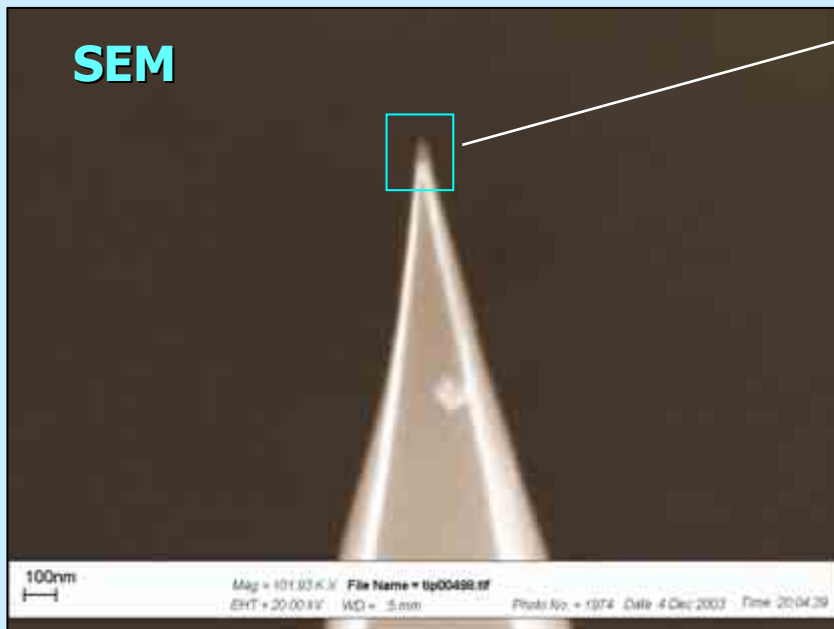
Atomic Force Microscope SOLVER P-47H

scan $47 \times 47 \mu\text{m}^2$



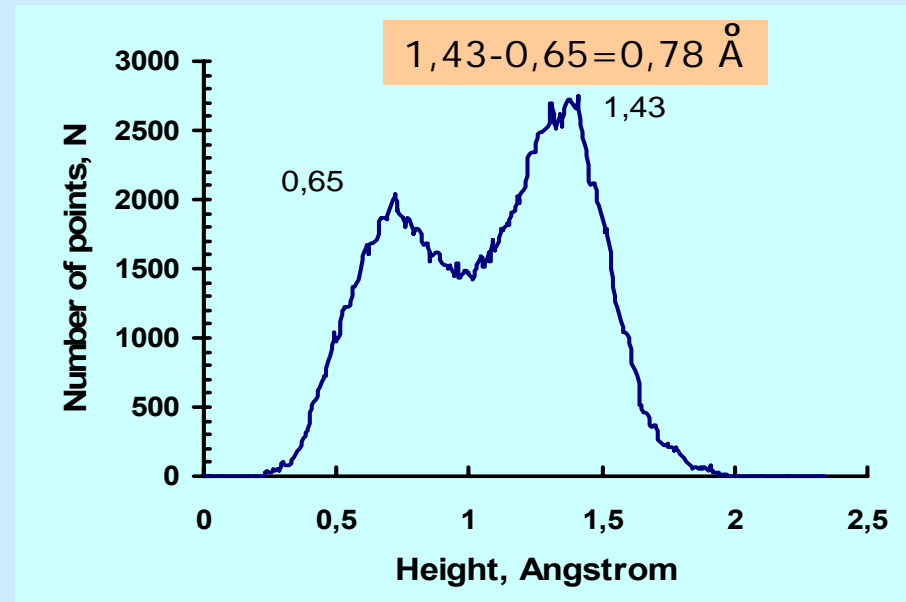
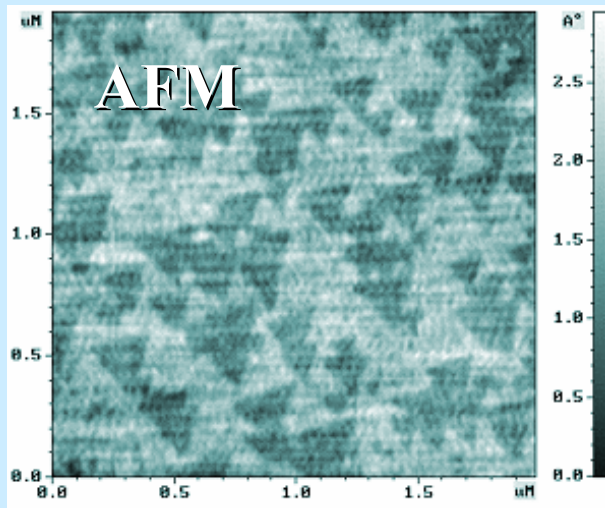
*Some example of AFM resolution –
monatomic steps, 0.14nm in height,
on silicon (001) surface*





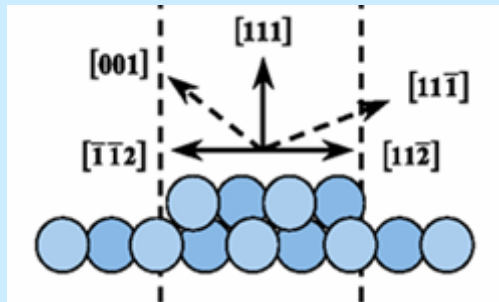
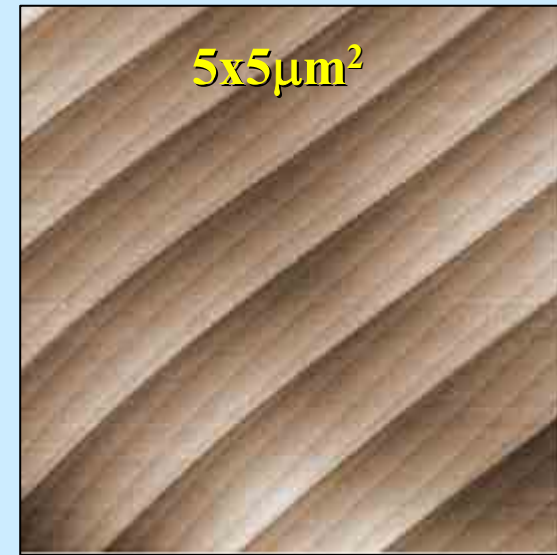
Scanning electron microscopy and high resolution transmission electron microscopy control of sharpness of Noncontact Silicon Cantilever for the best resolution

Test sample for resolution

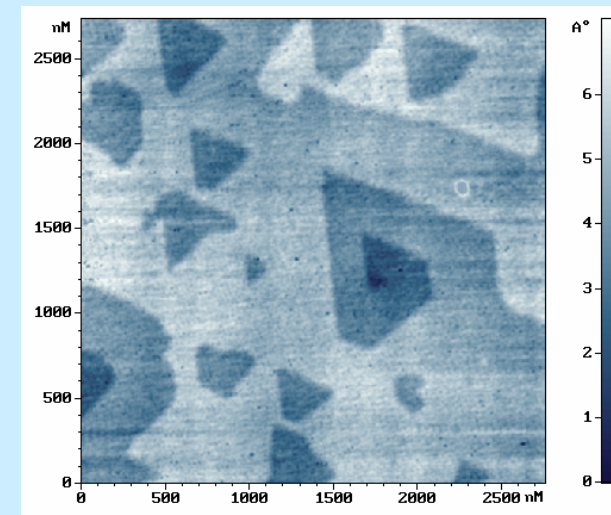


- Silicon (111) surface after quenching
- Structure of flat terraces
- Triangular areas are the (7x7) domains.
- White areas are the unreconstructed (1x1).

Analysis of step distribution on Si(111)

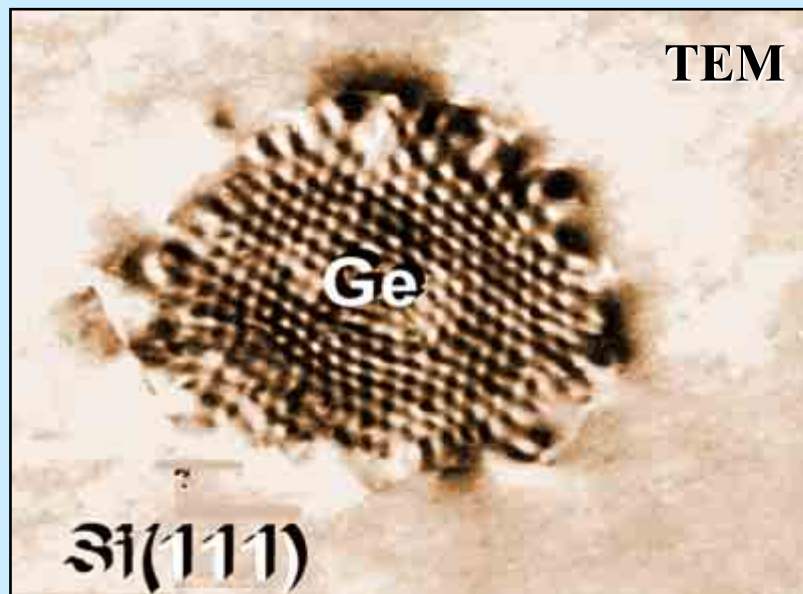
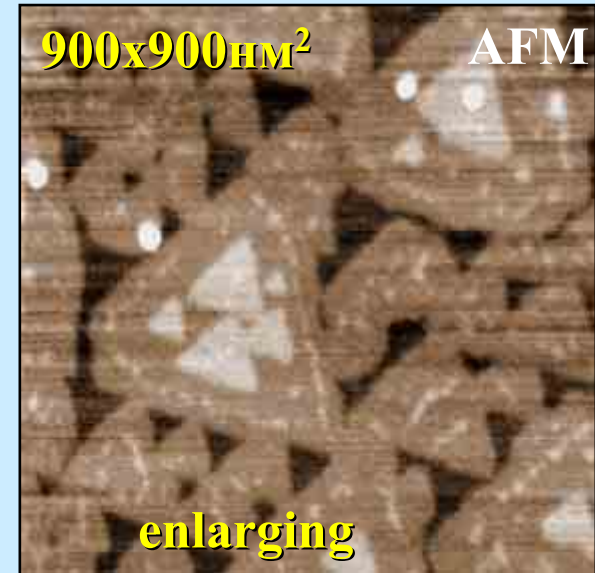
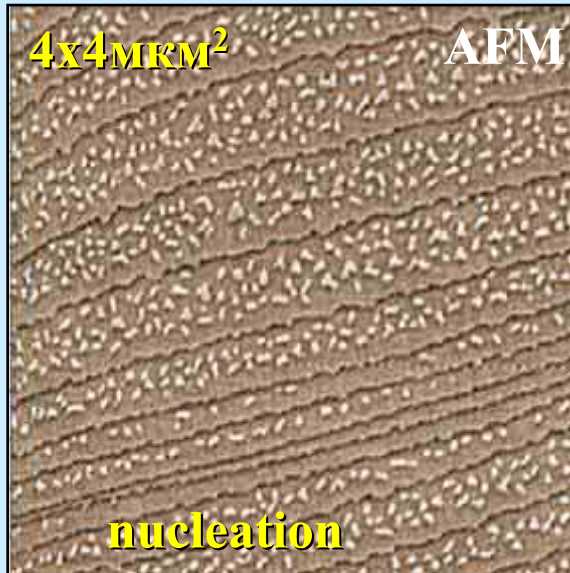


Typical ACM images and schematical representation of the surface with steps in height of one interplanes distances. To model the step motion in the frames of a linear kinetics approximation, one can take into account the changes in free energy.



Dislocation emerging at surface

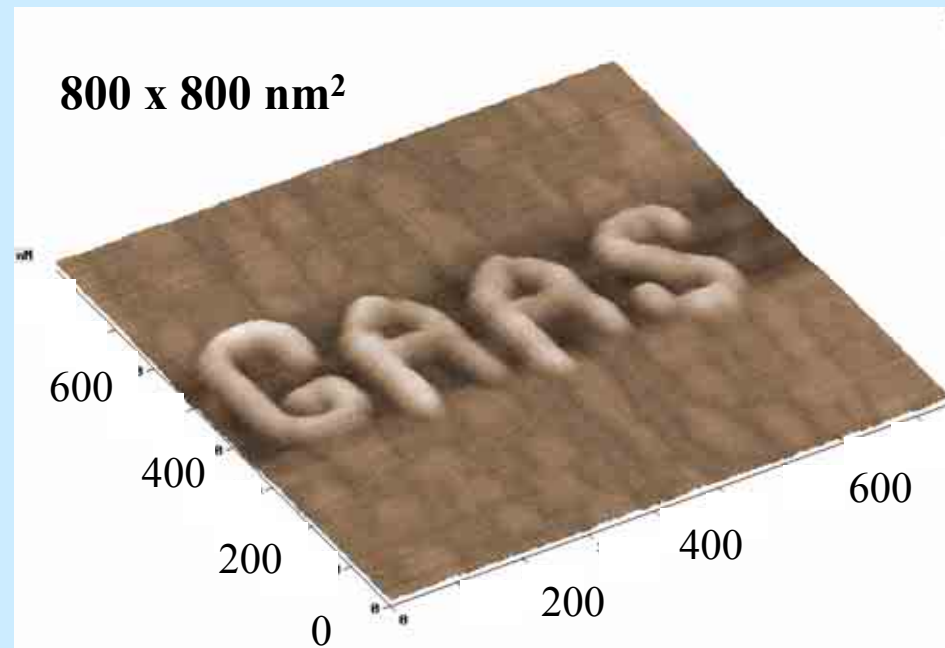
Analysis of structural-morphological peculiarities of low-dimensional system



AFM-images of initial stages of epitaxial growth germanium islands on silicon substrate. Size dependence and islands distribution were studied in details. Typical TEM-image of germanium island on the silicon (111) surface is presented also.

SPM-based nanofabrication

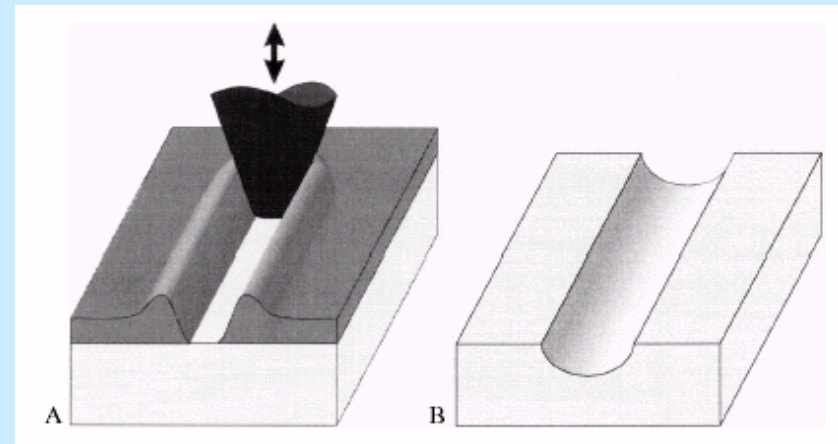
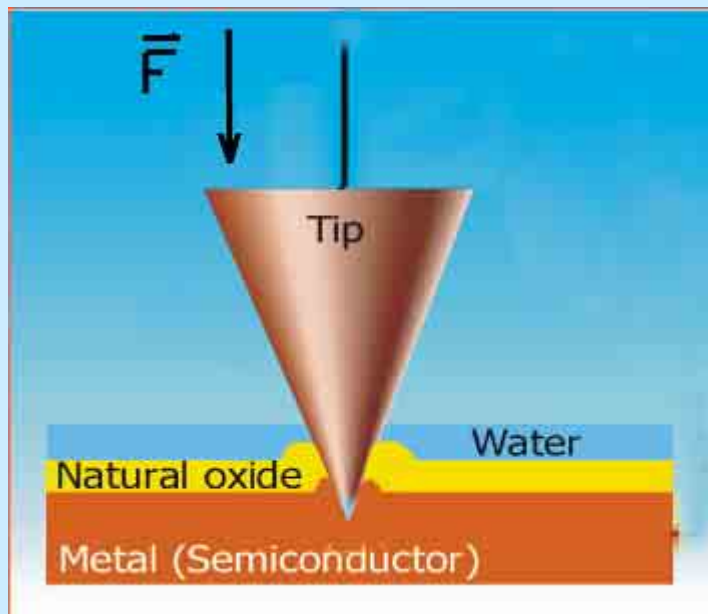
- single atom or molecules manipulation
(Rotation, Hopping, Dissociation, Assembling)
- magnetic reordering
- dynamic plugging
- local oxidation
- phase changing
- chemical activation
- Coulomb charging





Stress induced lithography

Precision mechanic stress induced by AFM tip as method of nanolithography

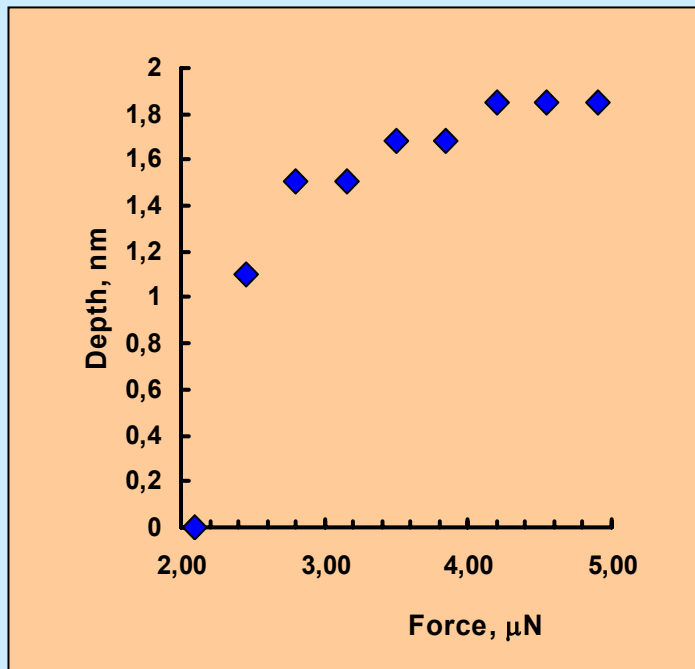


*D. Sarid, Scanning Force Microscopy
(Oxford University Press, Oxford, 1994)*

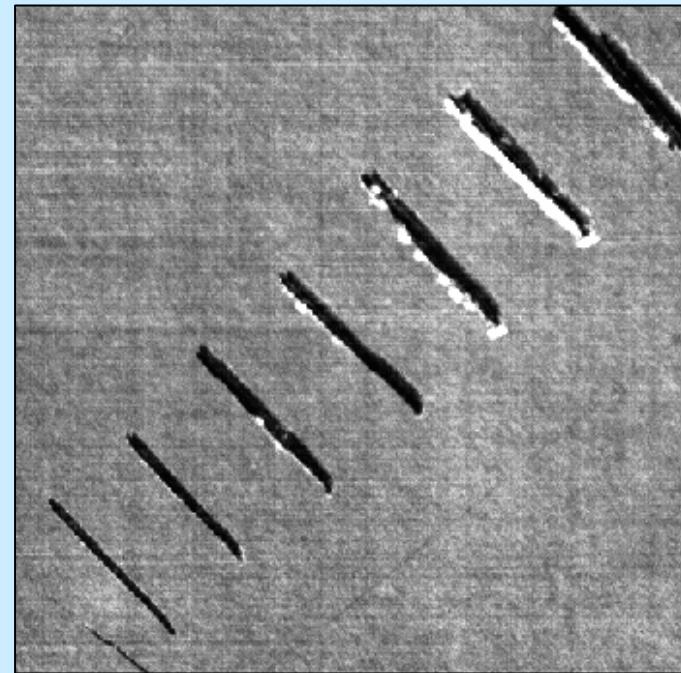
$$\vec{F}^{st}(r) = -\frac{2F_0^{st}}{3} \left(\left(\frac{\sigma}{r} \right)^2 - \frac{1}{30} \left(\frac{\sigma}{r} \right)^8 \right) \vec{r}$$

Lithography of mechanic scratching

dynamic destruction by means of mechanical stress during interaction between surface and AFM tip

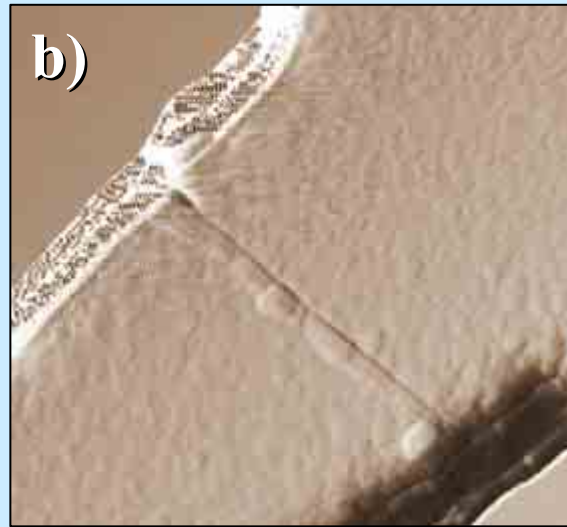
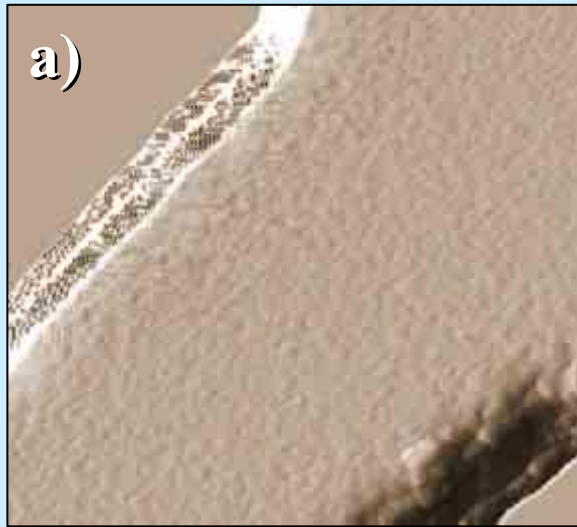


Dependence of the cut line depth on the interaction force between tip and surface.

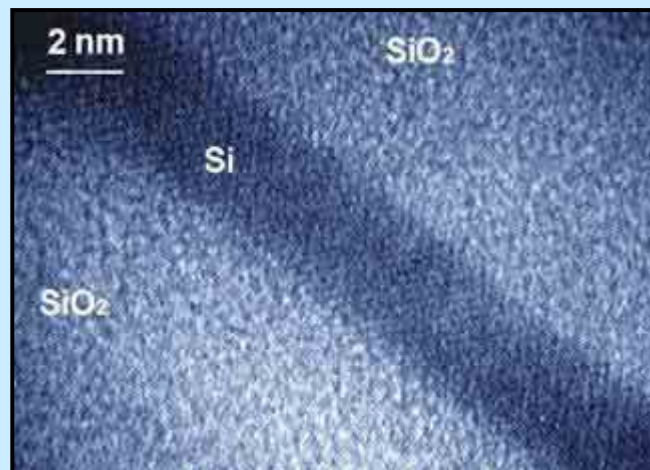
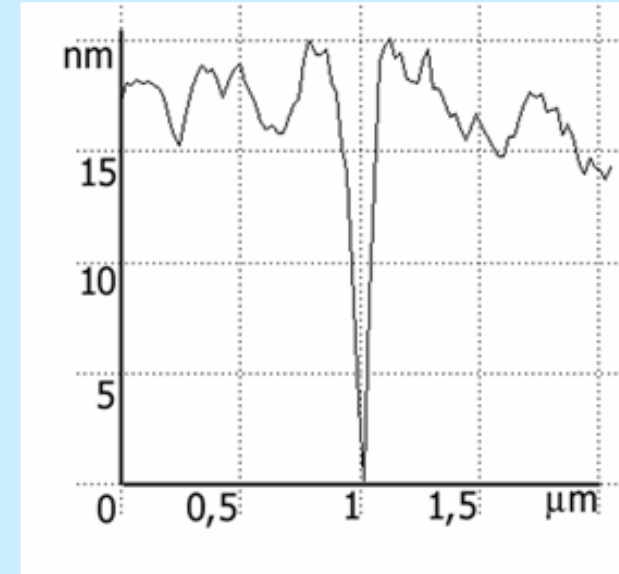


AFM topography of the GaAs (001) surface with set of cuts induced by AFM-tip scraping ($3 \times 3 \mu\text{m}^2$)

Silicon-on-isolator nanostructures



before (a) and after (b) AFM-tip scratching.



HREM-image of 3nm monocrystal silicon film of SOI (Dele-CUT technique).

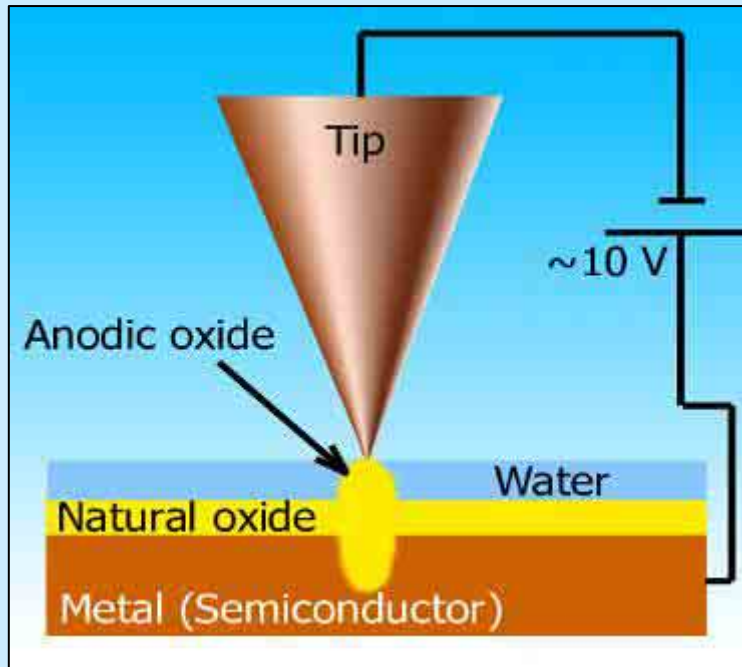


Y.V.Nastaushev et al., IEEE (2005).

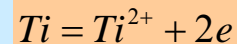
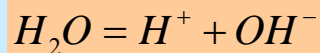
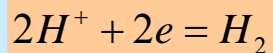


Local anodic oxidation lithography

Anodic oxidation under AFM tip as method of nanolithography



Atomic force microscopy becomes an important tool for imaging surface down to atomic scale even under atmospheric condition. The advantage of local anodic oxidation by means of atomic force microscope is possibility to modify semiconductor or metal surface locally at ambient condition. The characteristic size of nanomodification for this method varied from 1 to 100 nanometers.



$$J^{elec} = A' \exp\left[-\frac{h}{h_c}\right]$$

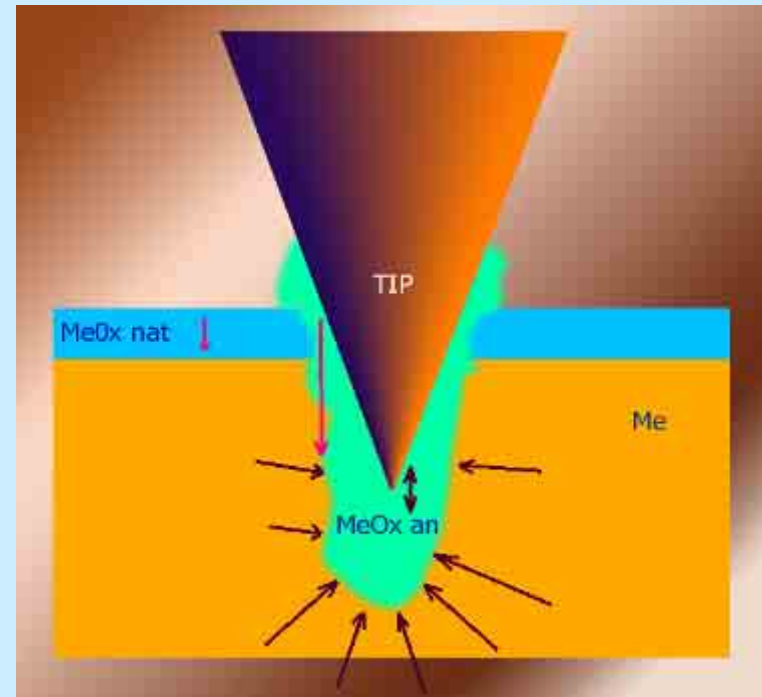
$$J = D \frac{\Delta N_{o-}}{h}$$

- **Natural oxide layer on the surface, which limits an anions diffusion to the bulk.**
- **Mechanical stress in the volume initiated by oxide growth, which limits cation diffusion to the reaction zone.**

$$E_s = \int_V \sum_{i,j=1}^3 0,5 \varepsilon_{ij} \sigma_{ij} dV = \frac{2Y}{1+\nu} \varepsilon_0^2 V$$

W.P.Gillin, D.J.Dunstan,
Phys.Rev.B., 50 (1994) 7495

- **Unstable oxidation at high potential difference between tip and substrate.**
- **Edge effects induced by limited shape of the tip and tip stability.**

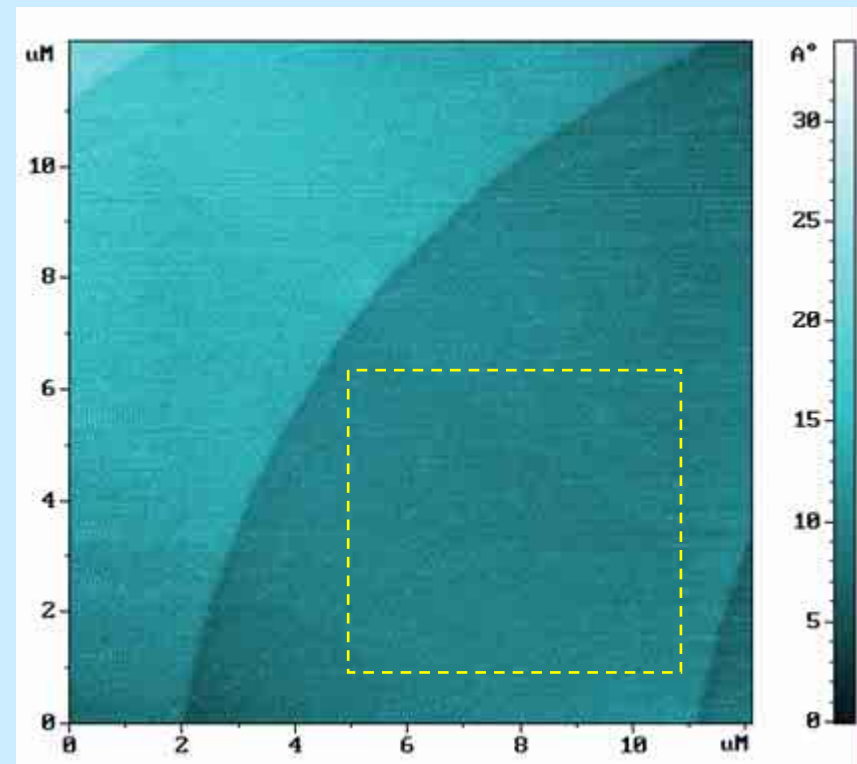




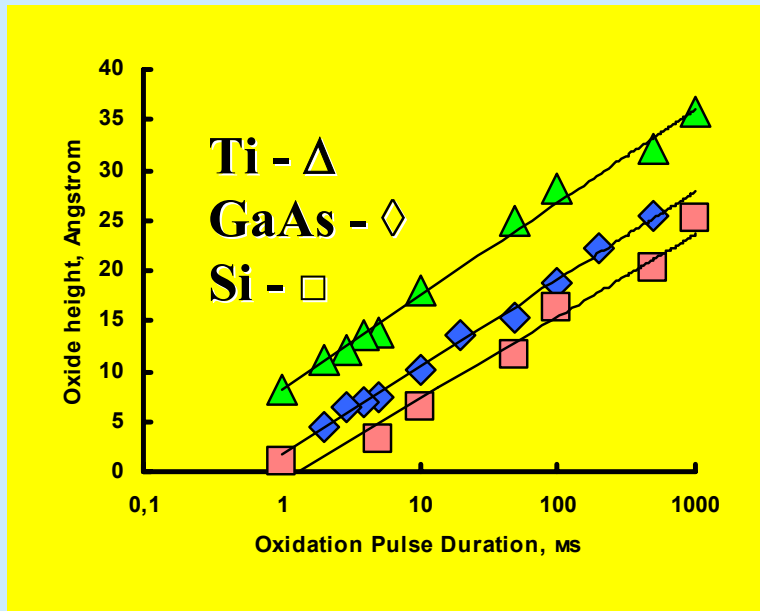
Large Terrace on Silicon Surface

- Surface : 5842.1 nm x 5895.9 nm
- Peak to peak, $R_{\max} = 5.952 \text{ \AA}^{\circ}$
- Mean, $R_{\text{mean}} = 5.581 \text{ \AA}^{\circ}$
- Roughness, $R_a = 0.587 \text{ \AA}^{\circ}$
- Root-Mean-Sq, $R_q = 0.723 \text{ \AA}^{\circ}$
- Skewness, $R_{\text{sk}} = -0.079$
- Kurtosis , $R_{\text{ku}} = 2.738$

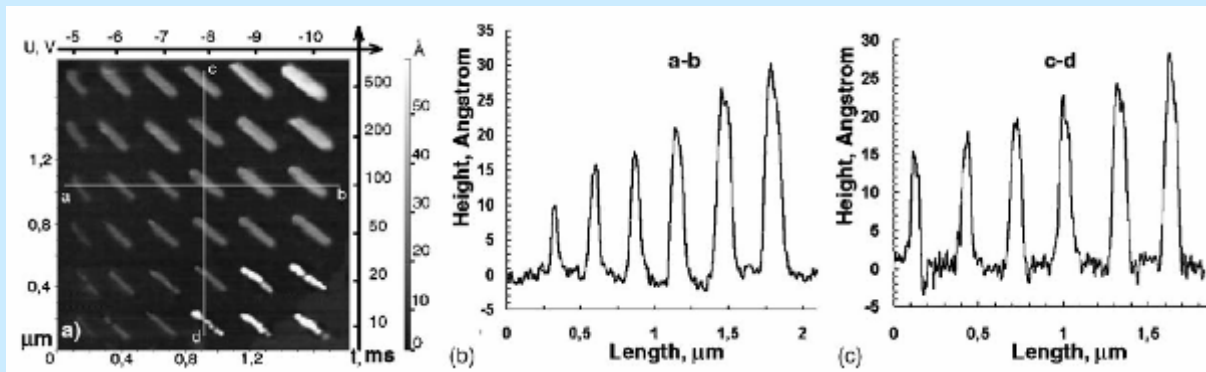
Typical AFM image of
Si(111) surface with
extremely wide terraces.



Height of Oxidation



	Ti	GaAs	Si
$h_c, \text{ nm}$	$0,41 \pm 0,06$	$0,38 \pm 0,06$	$0,36 \pm 0,06$
$\chi_0, \text{ meV}$	57 ± 14	66 ± 20	73 ± 24

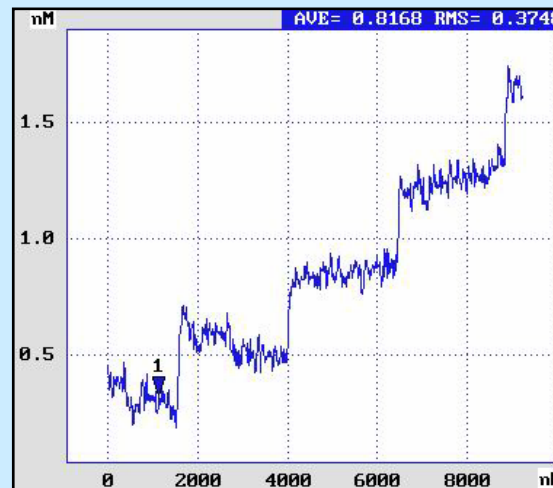
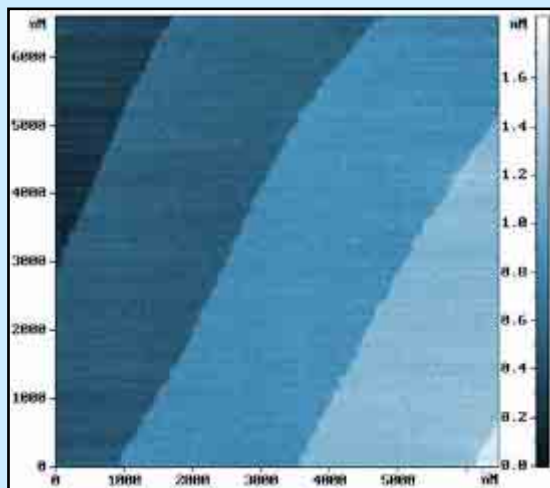
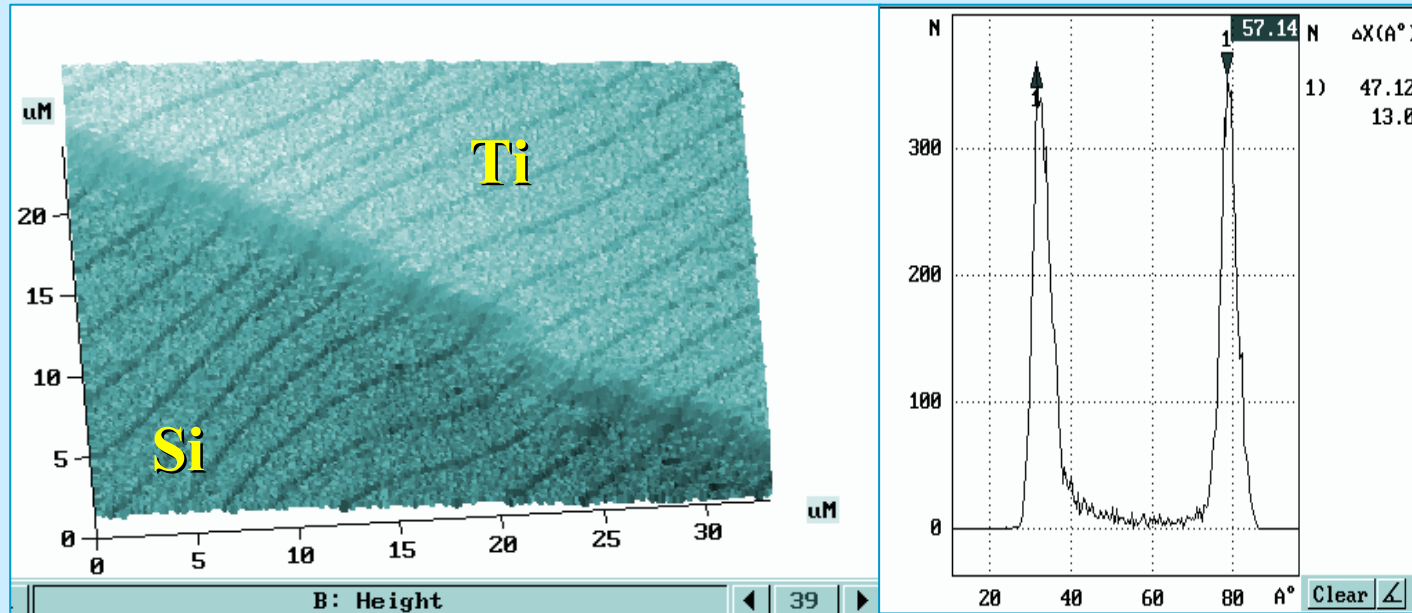


Electron percolation energies were estimated from threshold oxide height.

Topographical AFM-image of titanium film on the Si(111) substrate with the set of the anodic oxidized lines (a). The applied potential time and voltage magnitude were increased from bottom to top and from left to right, correspondingly. Relief profiles along the a–b (b) and c–d (c) lines.

$$h_c = \hbar(8m\chi_0)^{-\frac{1}{2}}$$

Titanium Film on Stepped Silicon Surface

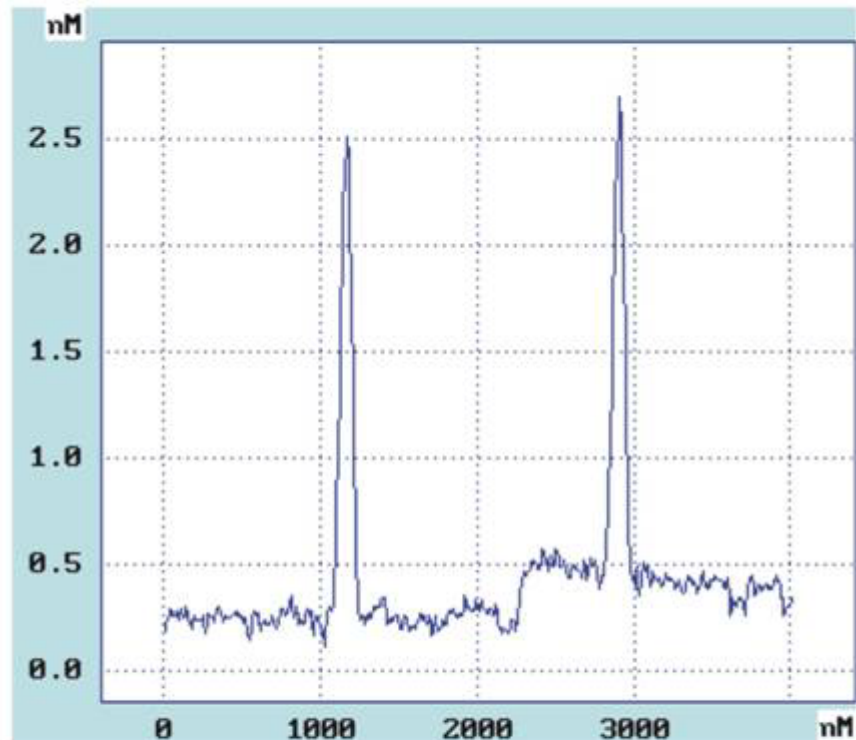
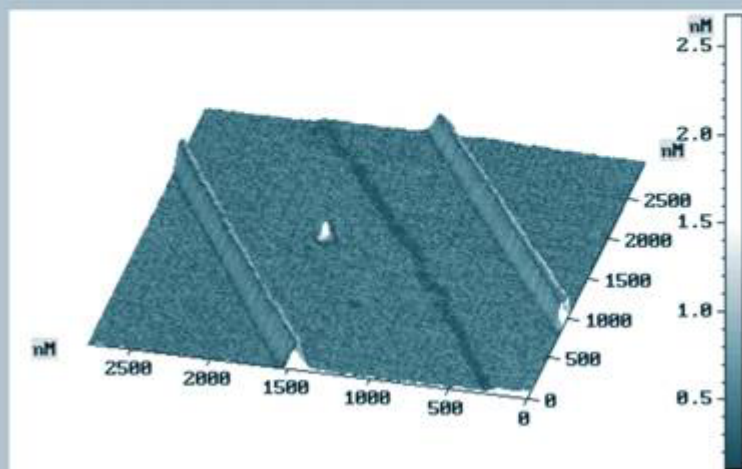
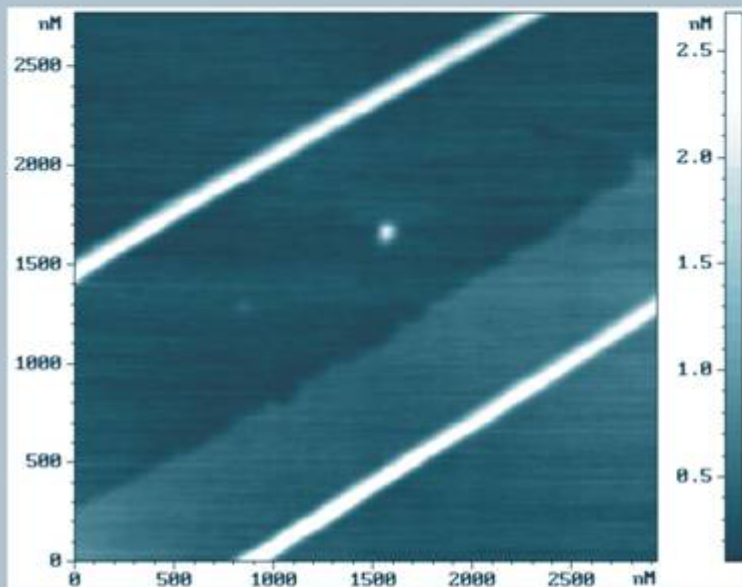


Titanium film replicates silicon monatomic steps (0,3nm).



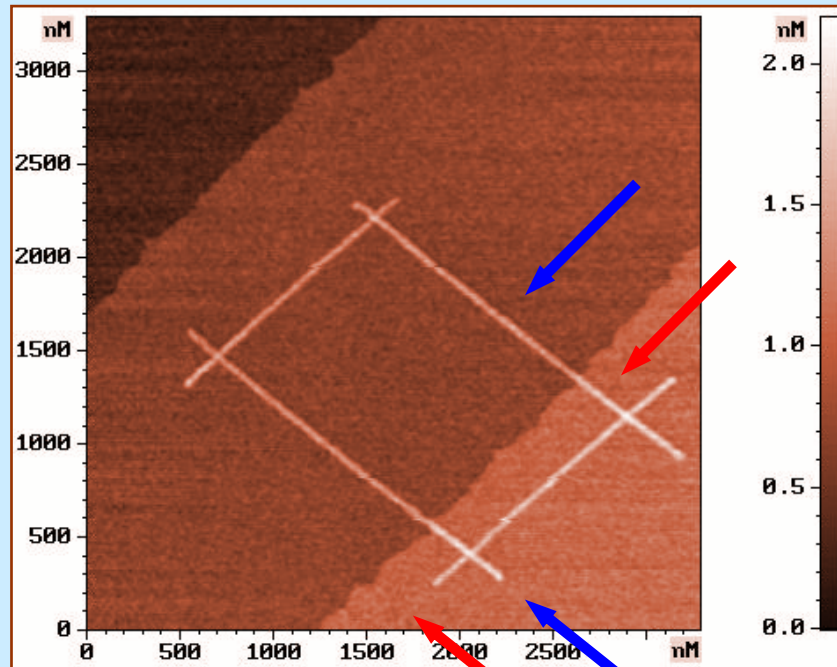
INSTITUTE OF SEMICONDUCTOR PHYSICS

RUSSIAN ACADEMY OF SCIENCES, SIBERIAN BRANCH

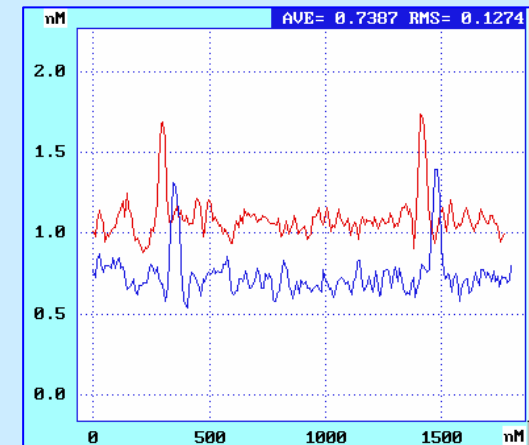


The lines of local oxidation using AFM probe on Si(111) surface with natural oxide and monoatomic step in central area (two-dimensional and three-dimensional images, and relief profile in the direction perpendicular to the lines as well)

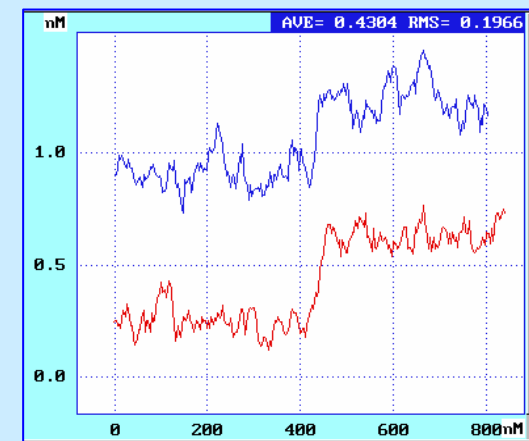
Peculiarities of nanomodification



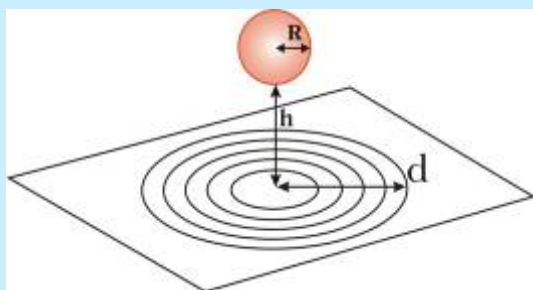
Topography 2D AFM-image



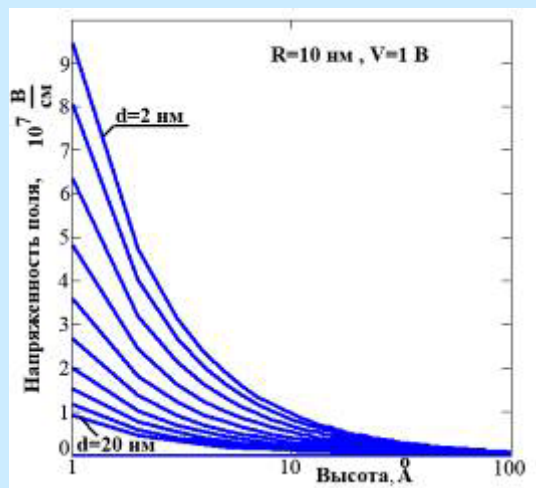
Topography cross-sections



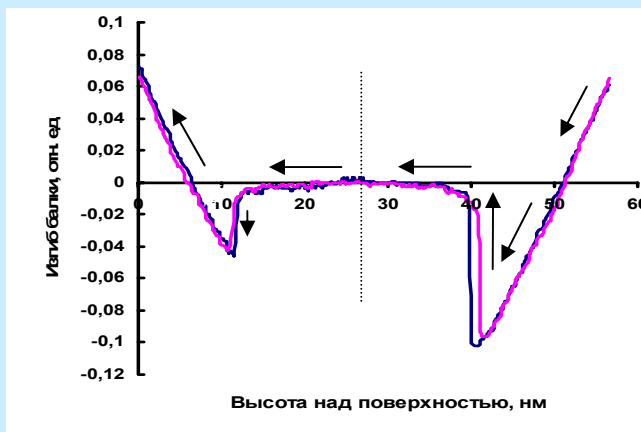
Optimization of tip-substrate interaction



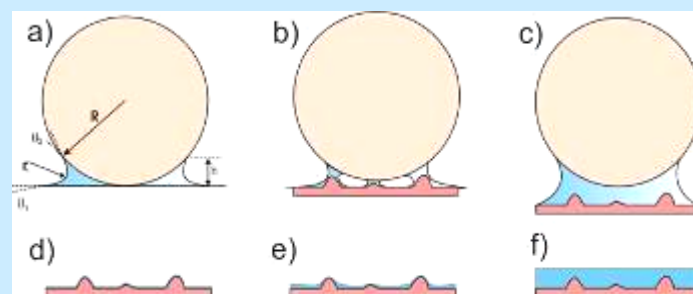
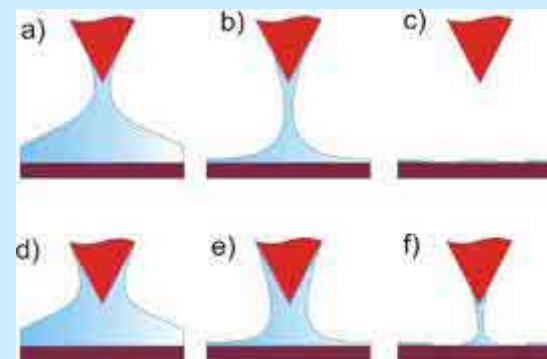
$$E = V \frac{R(R+z)(R+2z)}{z \left((R+z)^2 - d^2 \right)^{\frac{3}{2}}}$$



Simulation of electric field around a tip



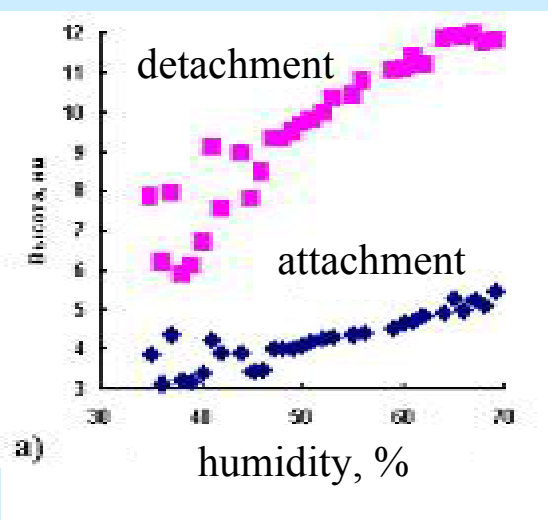
Interaction between tip and surface



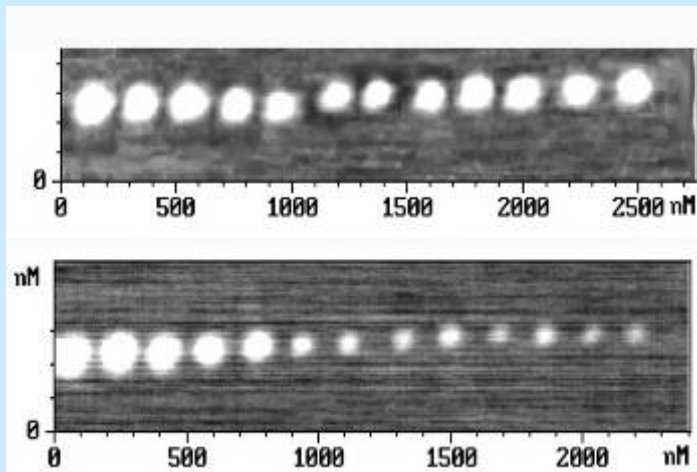
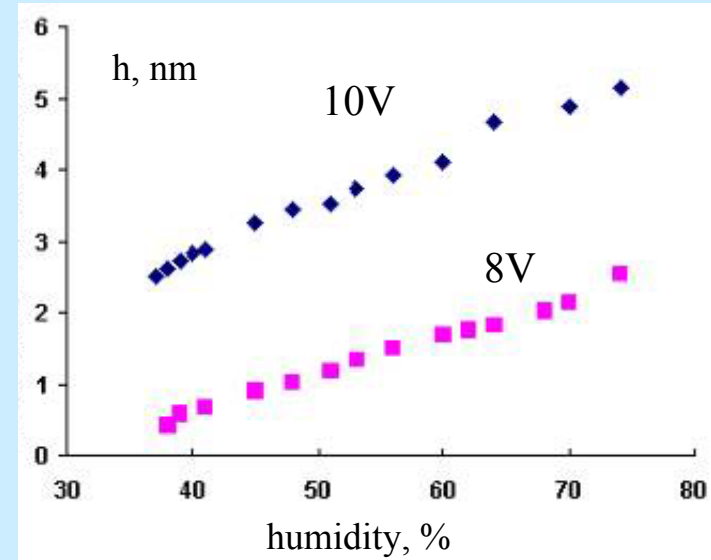
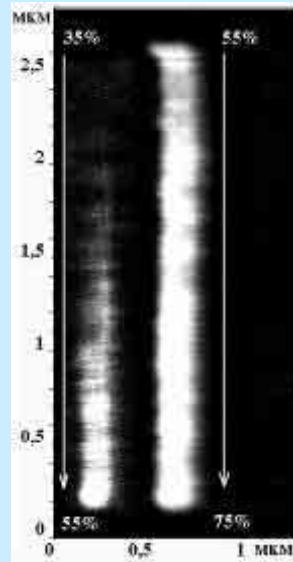
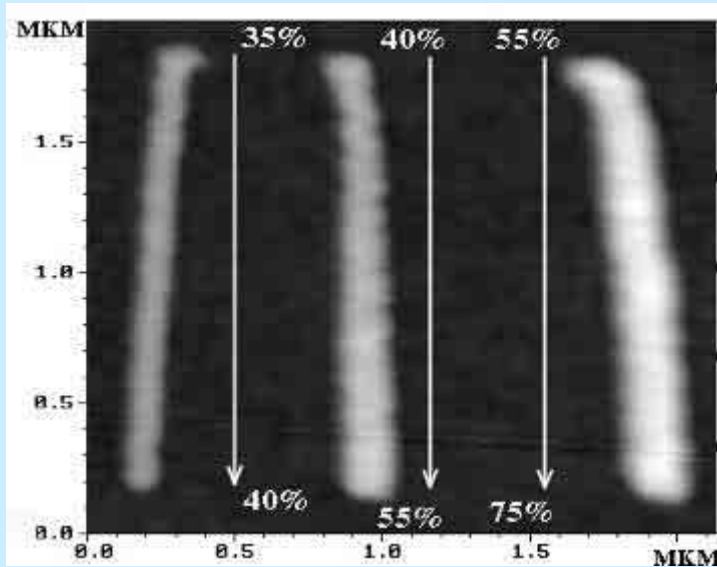
$$F_m = 2R\pi\gamma(\cos\theta_1 + \cos\theta_2)$$

$$4\pi\gamma \sum_i R_i \leq 4R_c\pi\gamma \quad F_m = 4R\pi\gamma$$

Contribution of adsorbed water

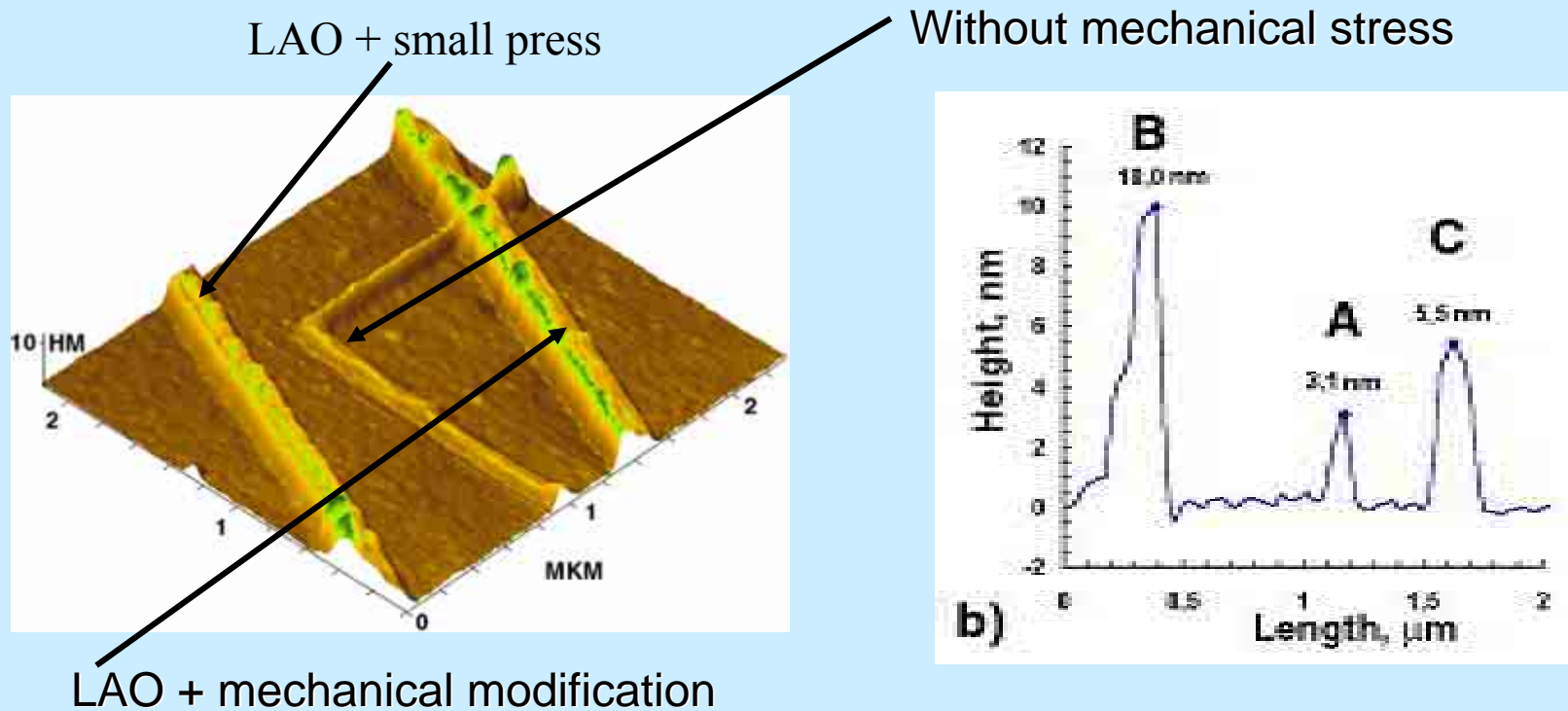


Line height as function of humidity



Local anodic oxidation produced by AFM-tip wasn't observed at ambient conditions with relative humidity less than 20-25%. With increasing of relative humidity up to 50%, the oxidation process was initiated but the permanent anodic oxidation occurred at relative humidity around AFM-tip more than 50%. To provide stable oxidation process, the experiments on titanium, silicon and gallium arsenic oxidation, presented in this paper, were carried out at 50-70% relative humidity.

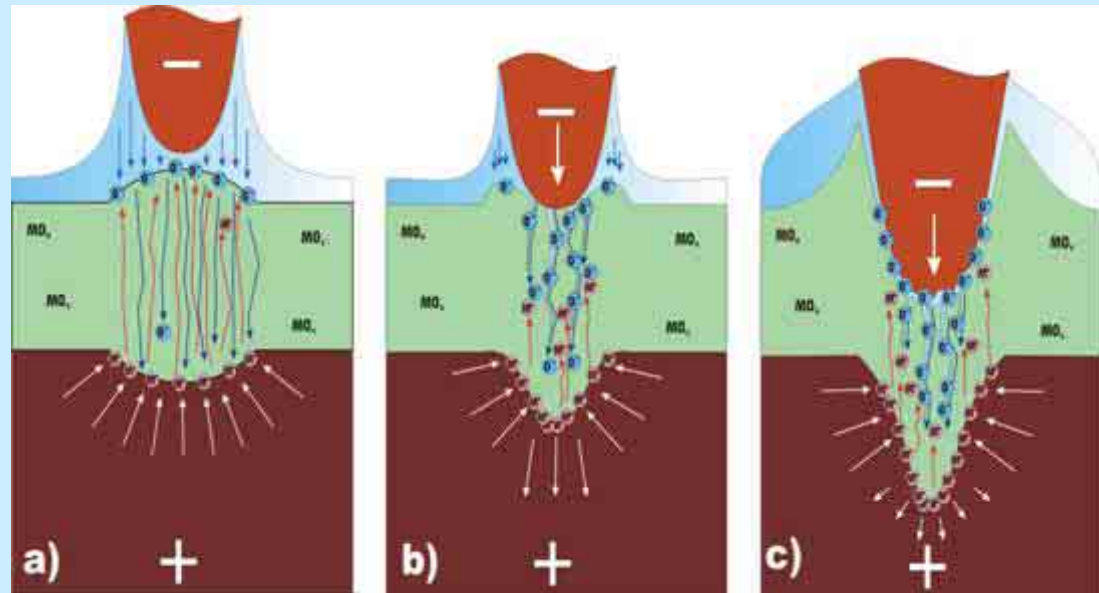
Nano-patterning on flat surfaces by AFM tip



The topographical AFM-image of GaAs surface with oxide lines which were obtained at same 10V potential but with different presses towards to surface. Line A is in 3,4 and 1,6 times less in height than line B and C respectively.

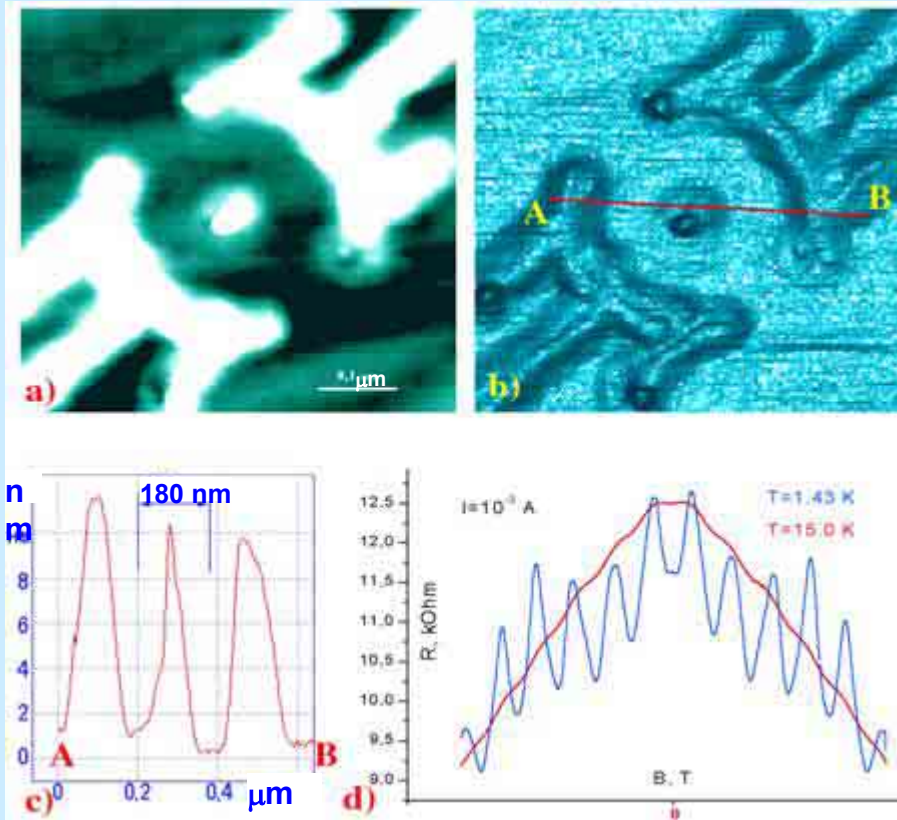
TINE&MEMO- technology of AFM- lithography

The new scale of depth of nanostructure fabrication was obtained (10-100 nm).



The novel technology of semiconductor nanostructure fabrication was developed on the base of simultaneous **Tip Induced NanoElectro & MEchanical MOdification (TINE & MEMO)**. Otherwise it was realized the method of simultaneous applying to the AFM-tip the both mechanical pressure and electrical bias in oscillation mode, which allows to destroy particularly a natural oxide layer on the surface and annihilate partly mechanical stresses in the substrate.

Aharonov–Bohm oscillation amplitude in small ballistic interferometers

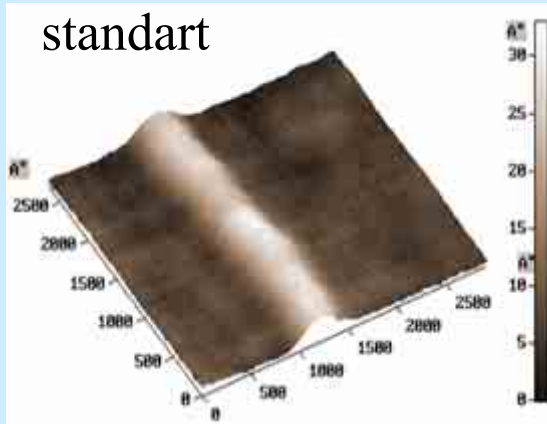


Topographical (a) and phase (b) AFM-images of the AlGaAs/GaAs heterostructure surface with the area modified by AFM-tip induced local anodic oxidation (quantum interferometer), relief profile along red AB-line (c). Aharonov-Bohm oscillations of the interferometer. The oscillation period $\Delta B = 0.16$ T corresponds to effective radius $r = 90$ nm.

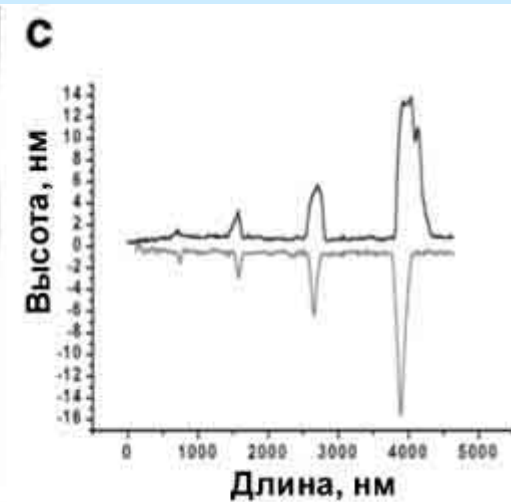
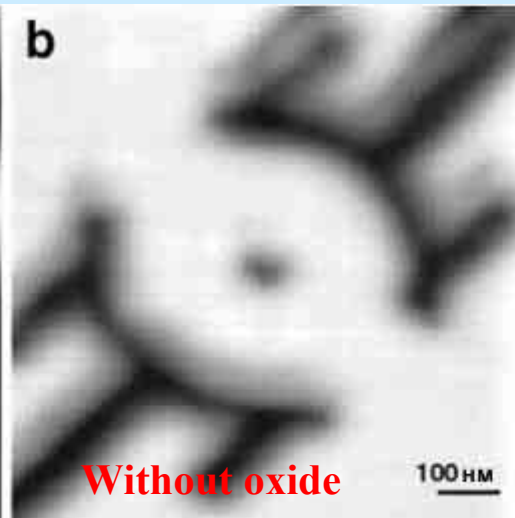
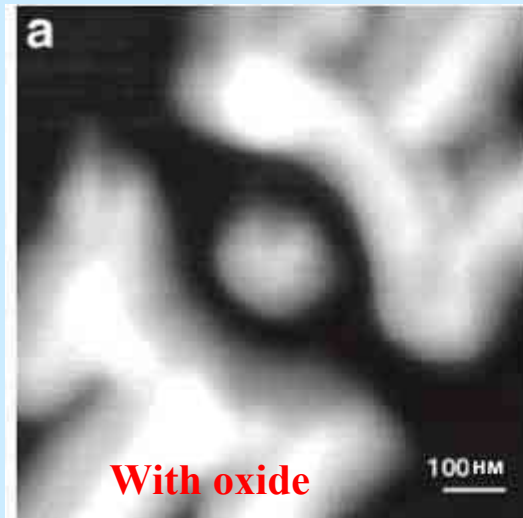
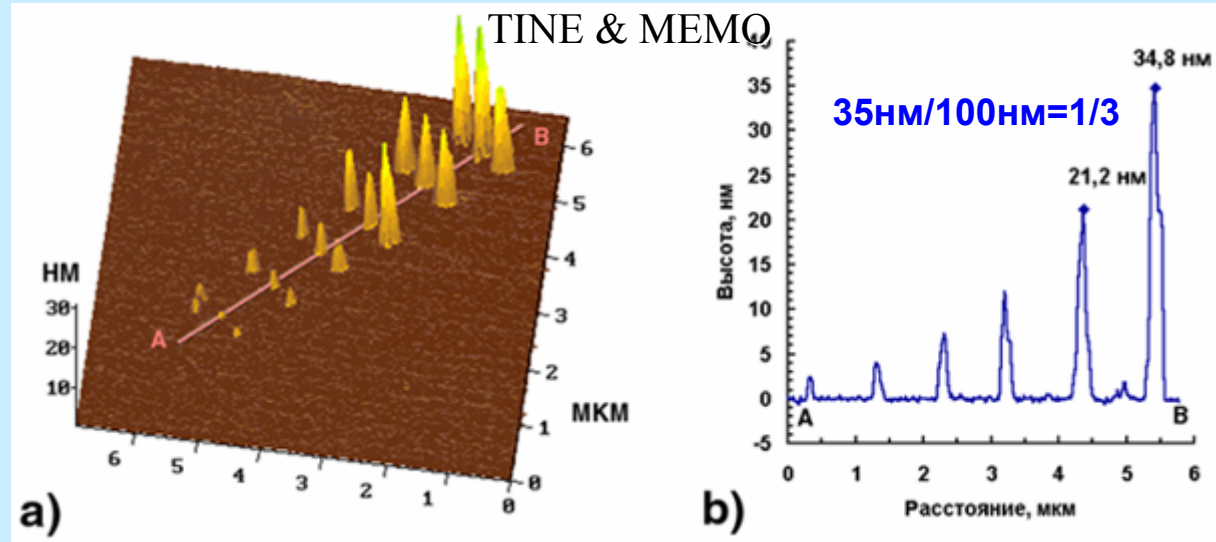
The principal new technology of semiconductor nanostructure fabrication was developed on the base of deep local anodic oxidation of titanium, gallium arsenide and silicon surfaces which was produced by conductive AFM-tip under applied additional potential. The new scale of nanostructures was obtained by this method (10-100nm). The quantum interferometer with an effective radius 90 nm was fabricated by nanoscaled AFM lithography. The small size of obtained structure allowed to increase the interferometer work temperature about one order (to 15 K).

Z.D.Kwon, D.V. Sheglov, A.V. Latyshev, E.B. Ol'shanetsky, V.A. Tkachenko, A.I. Toropov, A.L. Aseev, JETP Lett., Vol. 79, No. 3, 2004, p. 136.²⁶

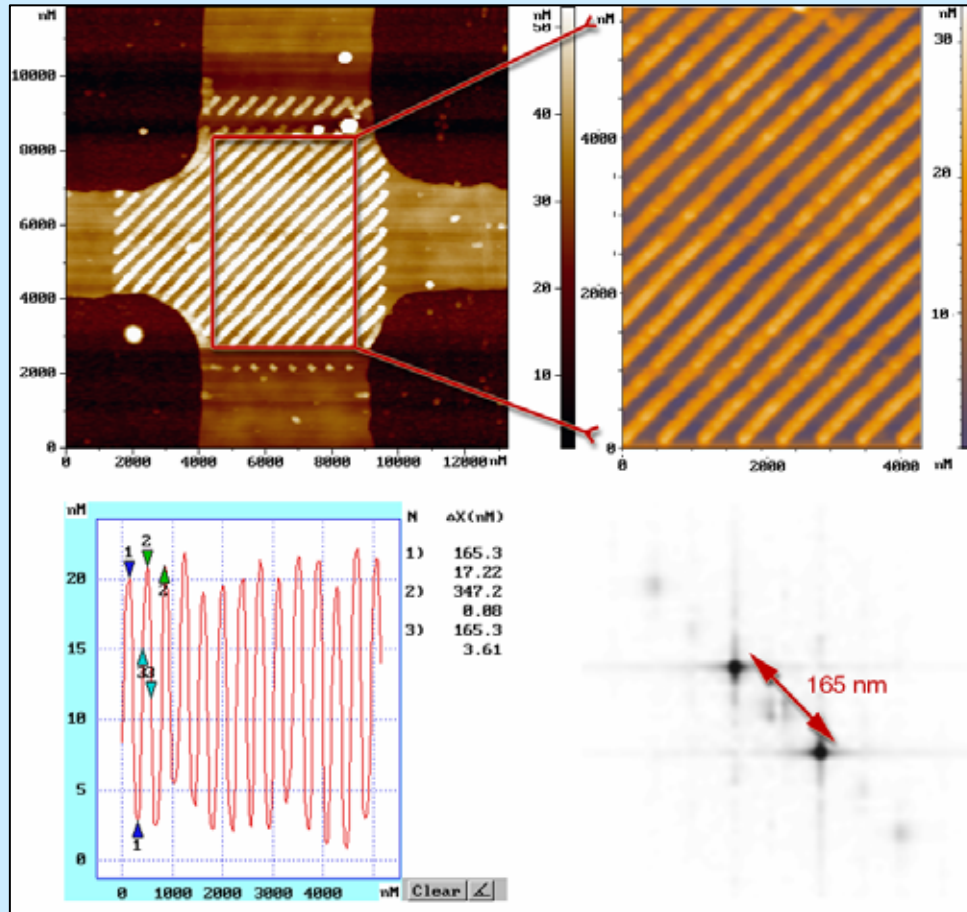
High aspect ratio (height/width)



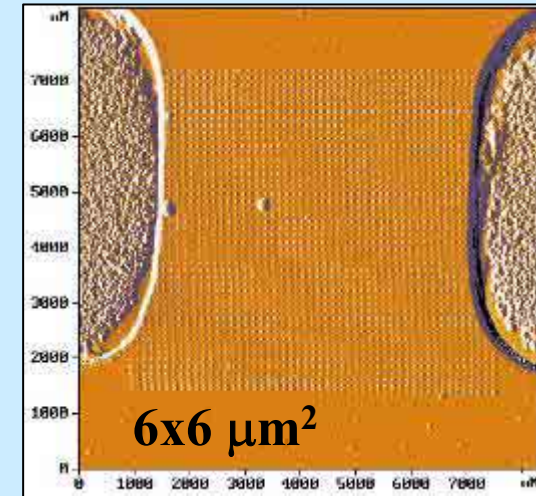
$$3,5\text{nm}/35\text{nm}=1/10$$



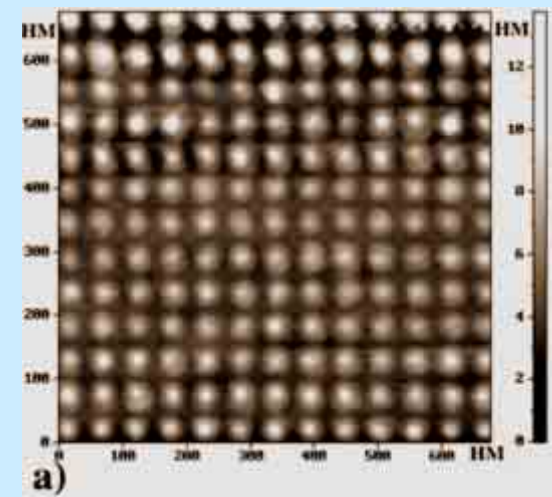
Nanoscale Patterning



SOI with the set of line (165nm)
multichannel FET
(10 nm SiO₂/ 44nm Si/ 327 nm SiO₂)

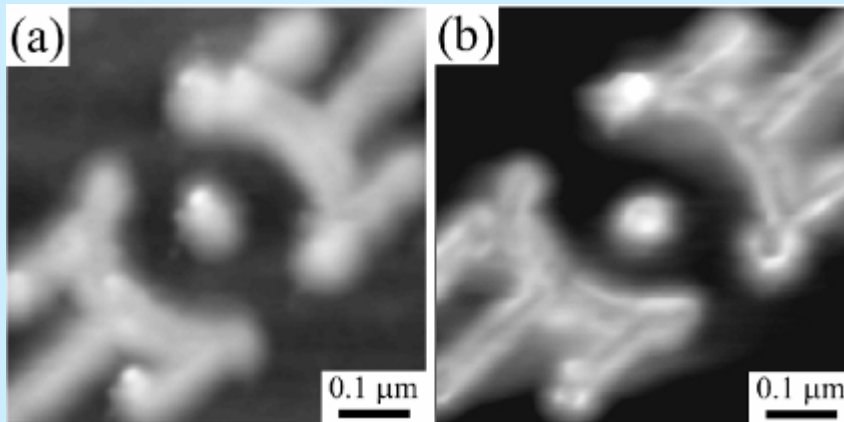


Set of dielectric points in TiN film

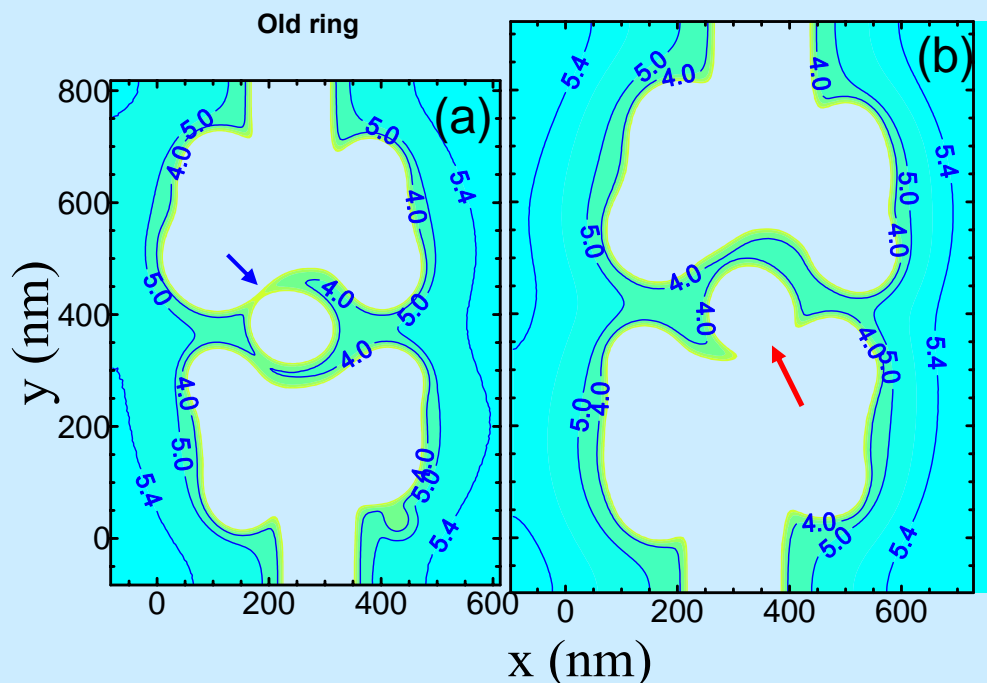


LAO points in GaAs

The effect of technological imperfections on the geometry of electron system



AFM images of open rings fabricated by the same lithographic pattern:
 (a) “symmetric” and (b) “asymmetric” rings.



Calculated 2D electron density distribution for the (a) symmetric and (b) asymmetric rings.

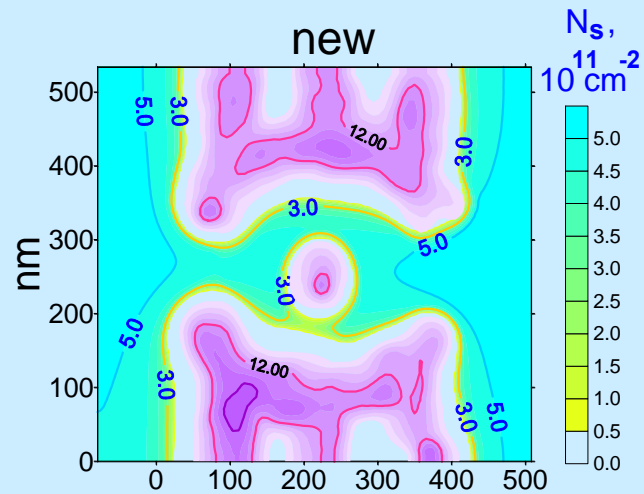
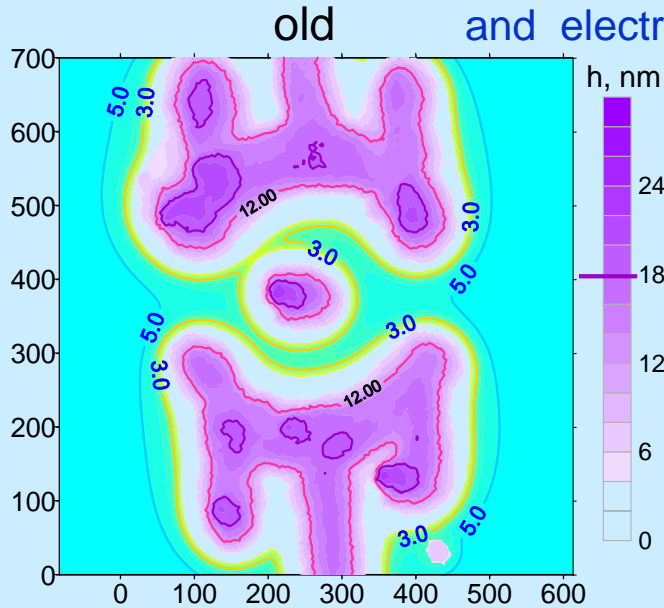
The rings appeared **broken** (b) or close to broken (a) even though the same lithographic pattern was used.

Breakdown of the electron ring due to depletion effect and random deviations from lithographic linewidth.

Numerical modelling of 3D electrostatics can help in optimizing the interferometer fabrication process.

Smallest ring interferometer (new) fabricated by local anodic oxidation

Map of the local anodic oxidation depth h and electron density N_s .

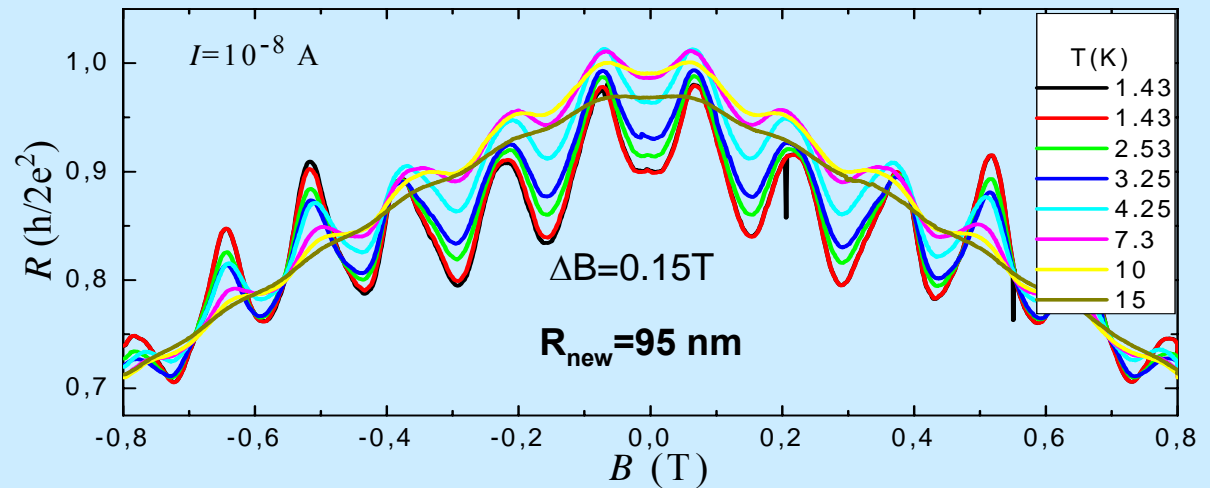


The depth of local anodic oxidation has been optimized to fabricate ring interferometers with radius < 100 nm.

Calculations based on AFM images of the samples provide extensive information about electron system of the interferometer and agree well with magnetotransport measurements.

The effective radius of the ring proved to be considerably larger than the antidot, which suggest an opportunity for optimization of the lateral oxidation pattern for further miniaturization of the ring.

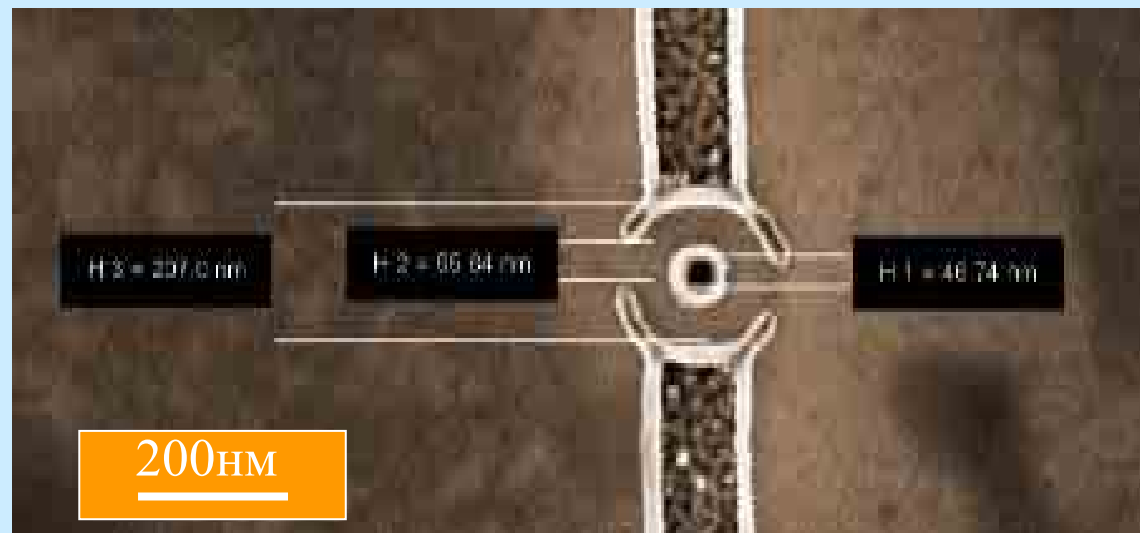
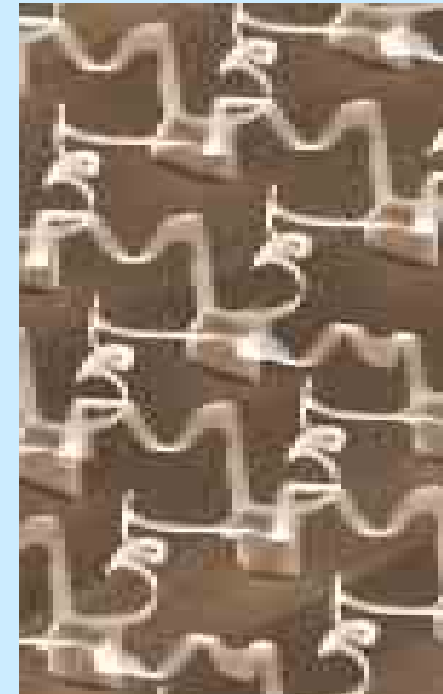
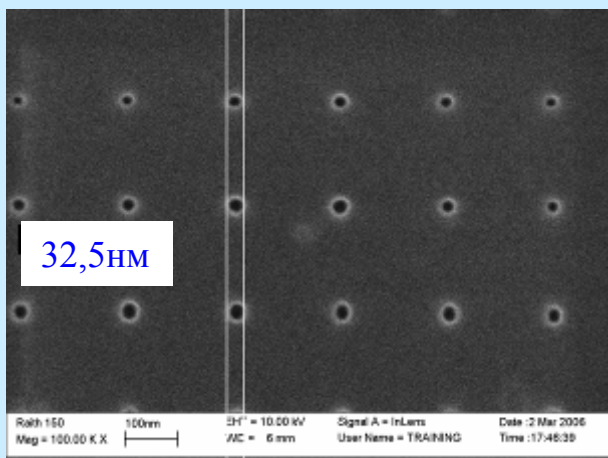
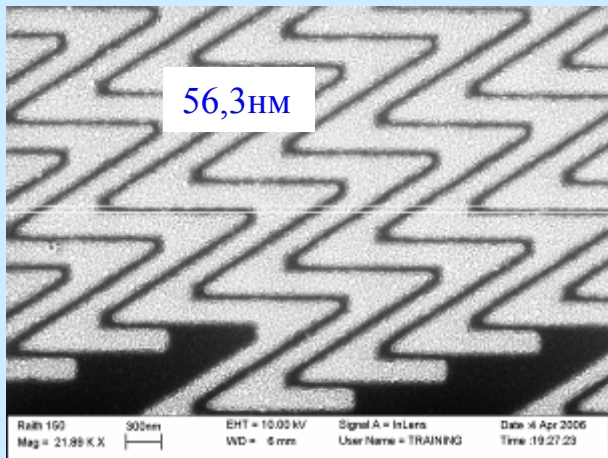
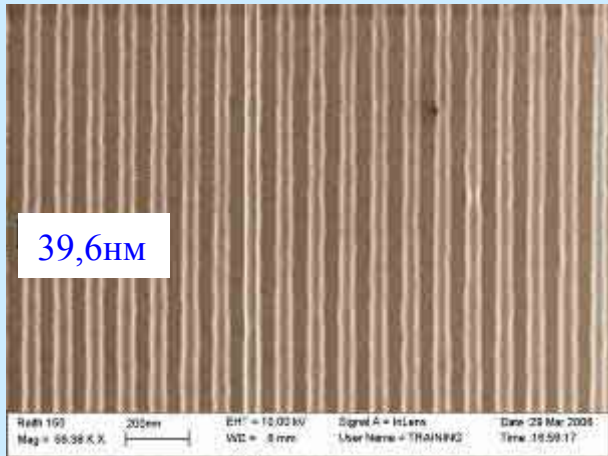
Measured resistance of the ring interferometers: Aharonov-Bohm oscillations



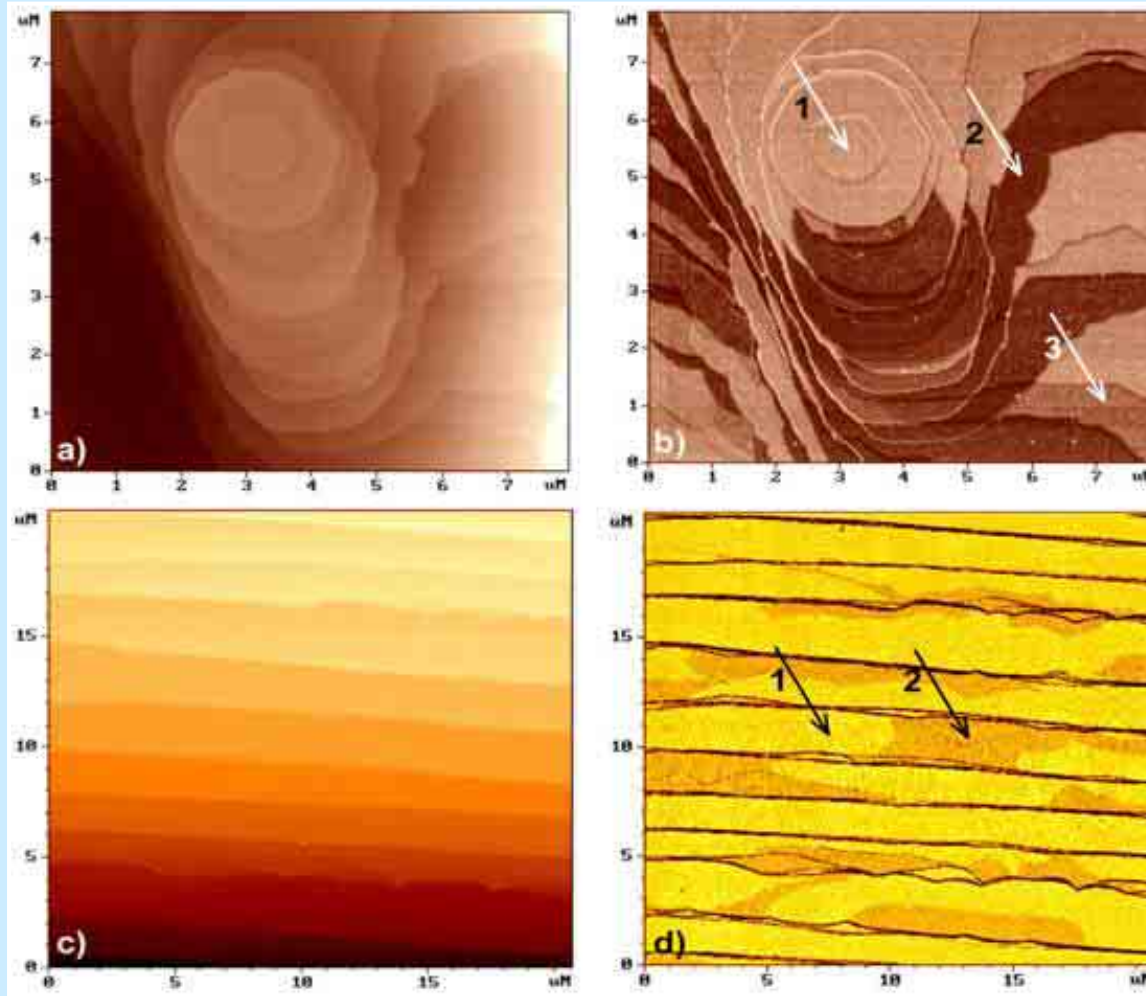
To fabricate a **new** sample the voltage on the AFM tip was reduced by factor of 2. The same lithographic pattern was used.

V.A. Tkachenko, D.V. Sheglov, Z.D. Kvon, Olshanetsky E. B. A.V. Latyshev, A.I. Toropov, O.A. Tkachenko, J.-C. Portal, A.L. Aseev. 14th Int. Symp. Nanostructures Physics and Technology, St. Petersburg, june 26-30, 2006, ND.13p

Nanolithography Raith 150



Application of AFM in Epitaxial Nanotechnology



Topographic (left) and phase contrast (right) AFM images of the silicon (111) surface after copper (top panel) and gold (bottom panel) deposition, respectively. Different phase contrast are marked by arrows.

CONCLUSION:

The obtained results provide the ground for development and application of nanoscaled lithography based on interaction between substrate and tip of atomic force microscopy.

The advanced TINE&MEMO technology is developed to realize the principle new scale of modification depth, up to 100 nm, for manufacturing electronic and mechanic nanodevices.

Calculations based on AFM images of the samples provide extensive information about electron system of the electronic devices.

The number of methodological recommendations for AFM based nanolithography was available.

